On mathematical modeling of epidermal wound healing

Jesse Kreger (Occidental College)

November 16, 2015

Abstract

In this paper we investigate two mathematical models of epidermal wound healing. The initial model, one reaction-diffusion partial differential equation (PDE) for cell density, was introduced by Jonathan Sherratt and James Murray in 1990. The second model, two coupled reaction-diffusion PDEs, includes an additional equation for the concentration of a mitosis regulating chemical. In this paper we discuss how the models arise from biological principles and then solve them numerically using the method of lines. We present analysis of asymptotic simplifications of the coupled reaction-diffusion PDE model and then show the existence of traveling wave solutions to both the simplified and full model. In conclusion, we discuss biological and clinical implications from the mathematical models.

Contents

1 Introduction

The initial model for epidermal wound healing was introduced by Jonathan Sherratt and James Murray in 1990 [14]. Since this time, the models have evolved to reflect increased mathematical and biological understanding of the process of epidermal wound healing. The focus of this paper is how these mathematical models developed over time. Furthermore, this paper will detail how a complex biomathematical model can not only be used to predict wound healing times, but also to provide biological insight into wound healing and perform 'mathematical experiments' that can have medical implications.

What is an epidermal wound?
An epidermal wound is a very common ailment that is often caused by a scrape or burn [11]. It is a surface wound to the skin; a wound is classified as an epidermal wound when the epidermis (surface layer of the skin) is injured but the dermis and flesh beneath the wound are not harmed. The biological processes driving the healing of such wounds are not completely understood. However, the mathematical modeling of epidermal wound healing can provide insight into these biological responses.

What is a mathematical model?
A mathematical model is a description of a system in terms of mathematical ideas and language. A mathematical model may not concern itself with every detail of a system (especially increasingly complex systems) but instead will take into account the overarching themes and structure of a system in order to produce some type of quantifiable results. A good mathematical model produces results that can provide insight into how the system operates and can be validated by comparing with actual data.

The epidermal wound healing mathematical model
The initial model of epidermal wound healing comes from a 1990 paper by British mathematical biologists Jonathan Sherratt and James Murray. Since then, numerous improvements have been made to this initial model. Completely new mathematical models have also been introduced. Overall, because epidermal wound healing is a complex process and such a common and pervasive affliction, it is a fantastic example of an area with a lot of potential for further analysis in both mathematical modeling and biological research.

2 Biology of epidermal wound healing

The epidermis is the thin outermost layer of cells in the skin, averaging only 0.775 mm [9]. In fact, the epidermis is so thin that in terms of the model, a sufficiently large epidermal wound can be approximated as two-dimensional. As soon as an epidermal wound occurs, platelets (blood cells) and fibrin (protein involved with clotting) gather at the wound and clot together so that the wound does not continue to bleed. Platelets are able to aggregate in a certain area and stick together due to the sticky fibrin proteins on their cell membranes. A biochemical signal is then released signifying that clotting has been successful and the wound can begin to heal. The process of epidermal wound healing is then characterized by three steps; inflammation, wound closure, and matrix remodeling in scar tissue. However, due to the overwhelming biochemical and biophysical complexity of wound healing, these steps are not fully understood [9].

During inflammation, the platelets release a number of substances that contribute to wound healing. These substances include: phagocytes (cells that ingest debris and bacteria in the wound), macrophages (secret growth factors that activate/inhibit mitosis), and other biochemical signals that alert the body about the wound. The critical goal of the inflammation process is to remove harmful substances from the wound and prepare it to be healed. For this reason, inflammation will continue until the wound is clean. If inflammation lasts for too long, the tissue near the wound can become damaged [5].

Wound closure for an epidermal wound consists only of epidermal migration, the movement of epidermal cells to the wounded area. This is because in the case of an epidermal wound, the dermis and other underlying structures of the skin are unwounded. Therefore, there is no need for wound contraction (which occurs in deeper wounds), thus greatly reducing the amount of biological and mathematical complexity. However, the means of epidermal migration are by no means well understood. Normal epidermal cells are not mobile. When a wound occurs, the cells on and near the boundary of the wound undergo a marked phenotype alteration called 'mobilization' that allows them to move. Cells can also come to the wounded area from the dermis such as from sebaceous glands, sweat-gland ducts, and hair follicles. The healthy epidermal cells then move into the wounded area to rebuild and cover the wound, a process know as re-epithelization. At first when the wound occurs, there is no immediate increase of cell mitosis and the cells continue to divide at a normal rate. However once enough cells have migrated to the wound boundary, the mitotic activity increases at the edges of the wound to about 15 times the normal rate. The main factors that determine this movement and replication are contact inhibition and biochemical effects such as growth factors and autoregulators. Contact inhibition is the process by which cells continue to replicate and move if they are surrounded by a sufficient amount of free space. However, if the cells are in regions of high cell density and they begin to hit other cells they stop replicating and moving. This helps ensure that the cells continue to grow in a single layer to re-cover the skin [7].

The purpose of the remodeling stage is to fix the originally disorganized healing that happens during wound closure. The proteins that were originally hastily laid down are rearranged and aligned along tension lines, i.e. rearranged to look like the skin that was there before the wound. Basically, during the remodeling stage a new skin layer forms over the healed wound returning the area back to its original state.

It is also relevant to introduce the difference between the activator and inhibitor chemicals, which will be important in the mathematical model. When an epidermal wound occurs and the cells have migrated to surround the wound, increased levels of the activator chemical are released to catalyze mitotic generation (increase the rate of mitosis). However, cell reproduction cannot indefinitely increase, which is why the inhibitory chemical is necessary. The inhibitory chemical completely shuts off a cell's ability to perform mitosis. As the chemical moves around, it slowly affects more cells thus reducing the overall mitosis rate.

Both chemicals are needed for wound healing, so that the cells can both multiply fast enough to cover the wound in a reasonable amount of time, but also so that there is some way to shut down the increased replication of cells around the wound once the wound is healed. If this did not occur then the cells would replicate as fast as possible indefinitely, leading to extra layers and tumors in the skin. This is also why it is biologically appropriate that the activator chemical has a much higher rate of decay than the inhibitor chemical [14].

It is clear to see that a mathematical model expressly incorporating each of the many factors

in wound healing will quickly become increasingly complex and convoluted. This paper will explore and document the various steps of the different models of epidermal wound healing and how each one attempts to successfully model this complex biological process as simply and efficiently as possible.

3 The beginning: a single reaction-diffusion equation for cell density

3.1 The first model equations

The pioneering work done in the field of mathematical modeling of epidermal wound healing is a 1990 paper by Sherratt and Murray [14]. In their paper, a single reaction-diffusion equation is presented for epidermal cell density, $n(\vec{x}, t)$. This initial equation is the starting point for the model and will develop into the basic building block for further mathematical development. The vector $\vec{x}$ represents the spatial coordinates of the wound. To begin, the authors only consider a radially symmetric geometry, meaning that $\vec{x}$ is simply the radius of the wound. The variable t represents time.

The authors first started with the assumption that the surface of the wound is barren (meaning it contains no epidermal skin cells) and that the wound begins to heal as epidermal cells diffuse to the wound and replicate via mitosis. Then, as soon as the cell density in the wound reaches a certain predetermined value (say 80% of the original cell density), the wound can be declared as healed. The goal of the model is to be able to predict the healing time of epidermal wounds. The model equation can be expressed very simply in word form as

$$\boxed{\text{rate of increase of cell density, } n} = \boxed{\text{cell migration}} + \boxed{\text{mitotic generation}}. \tag{1}$$

Sherratt and Murray chose to model the cell migration by a cell density dependent simple diffusive term. This can be mathematically represented by $D\nabla \cdot [(\frac{n}{n_0})^p \nabla n]$, where D and p are positive parameters and n_0 is the unwounded cell density. If $p = 0$, then the equation represents the familiar Fickian diffusion, whereas a positive p results in nonlinear diffusion. Biologically, this nonlinearity could represent the presence of contact inhibition that effects how the cells replicate and move through the wound [14, p.30]. The authors then modeled the mitotic generation term as Verhulst logistic growth with a positive logistic growth parameter, s. This is because in an unwounded setting, it is biologically appropriate for the cell density to grow logistically until it reaches its carrying capacity, n_0. Therefore the mitotic generation term can be represented mathematically as $sn(1 - (\frac{n}{n_0}))$. By substituting the mathematical pieces into the equation, Sherratt and Murray created the first epidermal wound healing mathematical model. It was one simple reaction-diffusion equation given by

$$\frac{\partial n}{\partial t} = D\nabla \cdot \left[\left(\frac{n}{n_0}\right)^p \nabla n\right] + sn\left(1 - \left(\frac{n}{n_0}\right)\right), \tag{2}$$

with initial condition $n(\vec{x}, 0) = 0$ for $\vec{x} \in \Omega$ (the wounded area) because of the assumption that the surface of the wound is completely barren with no remaining skin or epidermal appendages and boundary condition $n(\vec{x}, t) = n_0$ for $\vec{x} \in \partial\Omega$.

In the linear case (when $p = 0$) this partial differential equation becomes Fisher's equation, which has known traveling wave solutions [9]. In the nonlinear case (when $p > 0$) the model

is a nonlinear partial differential equation with no known or immediately apparent solutions. This led the authors to numerically solve this partial differential reaction-diffusion equation for biologically relevant parameters in both the linear and nonlinear cases. They obtained solutions that looked like "a front of epidermal cells moving into the wound" [14, p.31]. Intuitively, this is biologically appropriate and could be a relevant solution to the model. Further, they found that the speed of the front of cells moving into the wounded area was about $6 \cdot 10^{-2}$ mm per hour for linear diffusion but was about $9 \cdot 10^{-3}$ mm per hour for nonlinear diffusion, which compares well with experimental data of $8.6 \cdot 10^{-3}$ mm per hour found in a study by Van den Brenk [16] in 1956. This suggests that the nonlinear diffusion is a much better representation of epidermal wound healing than simple linear diffusion. However, the numerical solutions that Sherratt and Murray found, even in the nonlinear case, lacked a characteristic 'lag then linear phase'. This means that immediately after a wound occurs there is initially very little regeneration of the wound (the lag phase), followed by sudden linear healing of the wound (the linear phase). The 'lag then linear phase' characteristic of regeneration of a wound has been well documented in biological data and experimental studies such as Snowden 1984 [15].

3.2 Numerical solutions in the linear diffusion case (when $p = 0$)

We begin with the nondimensionalized Fisher-Kolmogorov equation in one dimension, given here as

$$\frac{\partial n}{\partial t} = D\frac{\partial^2 n}{\partial x^2} + n(1-n). \tag{3}$$

We use finite difference quotients with $i = 0, 1, .., N+1$ as the discretized space index ($x_i = i\Delta x$) and $j = 0, 1, ..., M+1$ as the discretized time index ($t_j = j\Delta t$) to rewrite Equation (3) as

$$\frac{n_i^{j+1} - n_i^j}{\Delta t} = D\frac{1}{(\Delta x)^2}\left(n_{i-1}^j - 2n_i^j + n_{i+1}^j\right) + n_i^j(1 - n_i^j).$$

Solving for n_i^{j+1} we have that

$$n_i^{j+1} = D\frac{\Delta t}{(\Delta x)^2}\left(n_{i-1}^j - 2n_i^j + n_{i+1}^j\right) + \Delta t n_i^j(1 - n_i^j) + n_i^j, \tag{4}$$

where $\Delta x = \frac{1}{N}$ is the spatial step and Δt is the time step. We can now use a Forward Euler marching scheme to compute solution curves at each successive time step.

We have the initial condition $n(x, 0) = 0$ inside the wound domain $[0, 1)$. We also have the Dirichlet boundary condition of $n(1, t) = 1$, for all t. On the left hand boundary, we set a no flux boundary condition of $n_x(0, t) = 0$. These conditions, along with the iterative step given by Equation (4) provide the full numerical scheme. The MATLAB code of this scheme is provided in Appendix A.1.

The most important consideration to run this numerical scheme is the Courant-Friedrichs-Lewy (CFL) condition. The CFL condition is a necessary condition for convergence and stability for the finite difference quotient scheme used [8]. In this case, the condition dictates that

$$\mu = \frac{D\Delta t}{(\Delta x)^2} \leq \frac{1}{2}. \tag{5}$$

In the code, the user inputs μ and Δx values. The code then computes Δt based on Equation (5). If the inputed value of $\mu \leq \frac{1}{2}$, the numerical scheme will converge. Figure 1 is a plot of numerical solutions to Equation (3) computed using the code. It is identical to the numerical solutions computed by Sherratt and Murray in [14].

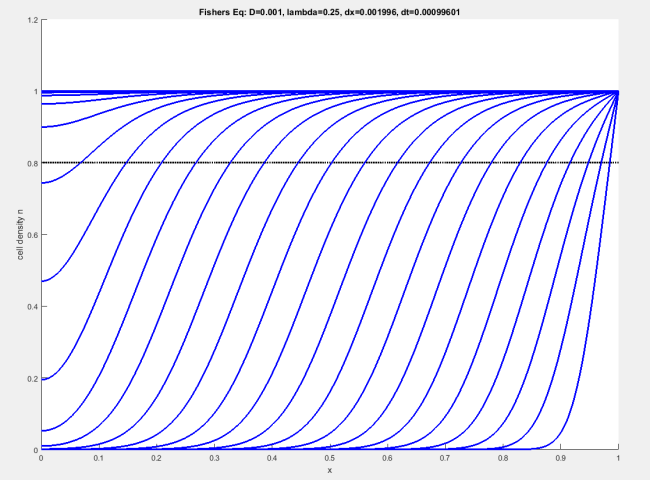

Figure 1: 1D Fisher-Kolmogorov numerical solutions (with $D = 10^{-3}$) at a selection of time steps with $\mu = 0.25, \Delta x = 0.001996$, and $\Delta t = 0.00099601$. The horizontal dotted line at $n = 0.8$ represents the predetermined cell density where the wound is declared healed. The traveling waves move from right to left.

To further understand how an epidermal wound heals, we can construct plots of the relationship between time and wound radius. To accomplish this, we simply find the vector entry in which each time step hits the critical 80% mark and divide that value by the total number of entries in the vector. This ratio is the amount that the wound has healed with respect to time. By doing this at each time step until the wound has completely healed, we get a curve that represents the relationship between time and wound radius. For the linear diffusion case, this curve is given in Figure 2. The MATLAB code implemented to make this Figure is given in Appendix A.2.

3.3 Numerical solutions in the nonlinear diffusion case (when $p > 0$)

We begin with the nondimensionalized Fisher-Kolmogorov equation with nonlinear diffusion in one dimension, given again as

$$\frac{\partial n}{\partial t} = D\frac{\partial}{\partial x}\left((n^p)\frac{\partial n}{\partial x}\right) + n(1-n), \tag{6}$$

with $p > 0$.

We use finite difference quotients with $i = 0, 1, .., N+1$ as the discretized space index and

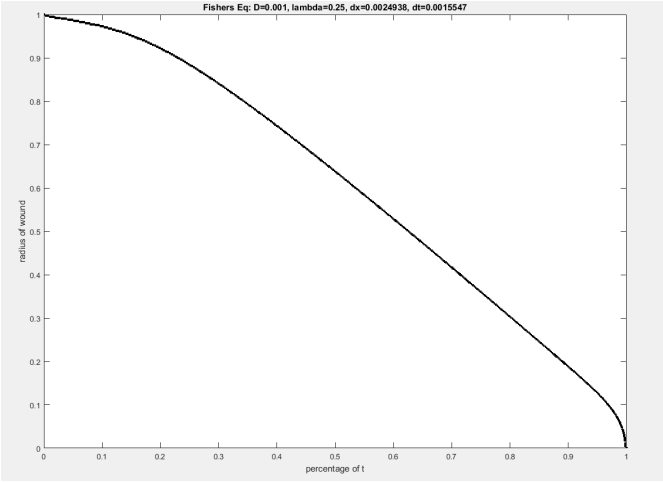

Figure 2: Time versus wound radius graph for the linear diffusion case. The x-axis represents the percentage of the total time that the wound takes to heal and the y-axis represents the wound radius in non-dimensionalized coordinates.

$j = 0, 1, ..., M+1$ as the discretized time index to rewrite Equation (6) as

$$\begin{aligned}\frac{n_i^{j+1} - n_i^j}{\Delta t} &= D\frac{1}{\Delta x}\Big[\Big(n^p\frac{\partial n}{\partial x}\Big)^j_{i+1/2} - \Big(n^p\frac{\partial n}{\partial x}\Big)^j_{i-1/2}\Big] + n_i^j(1-n_i^j)\\ &= D\frac{1}{\Delta x}\Big((n^j_{i+1/2})^p\frac{n_{i+1}^j - n_i^j}{\Delta x} - (n^j_{i-1/2})^p\frac{n_i^j - n_{i-1}^j}{\Delta x}\Big) + n_i^j(1-n_i^j)\\ &= D\frac{1}{(\Delta x)^2}\Big[\Big(\frac{n_{i+1}^j + n_i^j}{2}\Big)^p(n_{i+1}^j - n_i^j) - \Big(\frac{n_i^j + n_{i-1}^j}{2}\Big)^p(n_i^j - n_{i-1}^j)\Big] + n_i^j(1-n_i^j).\end{aligned}$$

It is important to note that p is an exponent (of nonlinear diffusion) and i, j are index markers. Also, points at the midpoints of spatial intervals such as at the $i + 1/2$ index are calculated as an average of the surrounding i and $i + 1$ points. For example,

$$n^j_{i+1/2} = \frac{n_i^j + n_{i+1}^j}{2}.$$

Solving the above for n_i^{j+1} we have that

$$n_i^{j+1} = D\frac{\Delta t}{(\Delta x)^2}\Big[\big(\frac{n_{i+1}^j + n_i^j}{2}\big)^p(n_{i+1}^j - n_i^j) - \big(\frac{n_i^j + n_{i-1}^j}{2}\big)^p(n_i^j - n_{i-1}^j)\Big] + (\Delta t)n_i^j(1-n_i^j) + n_i^j, \quad (7)$$

where $\Delta x = \frac{1}{N}$ is the spatial step and Δt is the time step. We can now use a Forward Euler marching scheme to compute solution curves at each successive time step.

We have the initial condition $n(x, 0) = 0$ inside the wound domain $[0, 1)$. We also have the Dirichlet boundary condition of $n(1, t) = 1$, for all t. On the left hand boundary, we set a no flux boundary condition of $n_x(0, t) = 0$. These conditions, along with the iterative step given by Equation (7) provide the full numerical scheme. The MATLAB code of this scheme is provided in Appendix A.3.

Similarly to the linear case, we need to satisfy the CFL condition [8]. In this case, the condition dictates that

$$\mu = \frac{D\Delta t}{(\Delta x)^2} \leq \frac{1}{2}. \tag{8}$$

In the code, the user inputs μ and Δx values. The code then computes Δt based on Equation (8). If the inputed value of $\mu \leq \frac{1}{2}$, the numerical scheme will converge. Figure 3 is a plot of numerical solutions to Equation (3) computed using the code. It appears identical to the numerical solutions computed by Sherratt and Murray in [14].

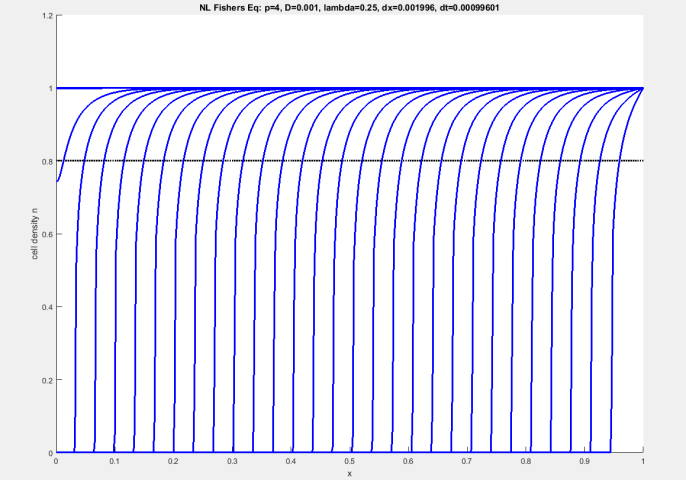

Figure 3: 1D Fisher-Kolmogorov with nonlinear diffusion numerical solutions (with $D = 10^{-3}$) at a selection of time steps with $p = 4, \mu = 0.25, \Delta x = 0.001996$, and $\Delta t = 0.00099601$. The horizontal dotted line at $n = 0.8$ represents the predetermined cell density where the wound is declared healed. The traveling waves move from right to left.

We can again make a time versus wound radius graph in the same method as before. This graph is given in Figure 4 and the code used to make it is given in Appendix A.4. The time versus wound radius graphs given by Figures 2 and 4 appear identical to the same graphs produced by Sherratt and Murray.

4 An improved model: a pair of reaction-diffusion equations for cell density and biochemical concentration

4.1 The improved model equations

The fact that the one equation model provided a much better fit to experimental data for nonlinear diffusion and the lack of a lag phase that has shown to be necessary in experimental data motivated the need to improve the model, specifically the need to incorporate a biochemical regulation mechanism. Simply put, Sherratt and Murray determined that "biochemical mediators are fundamental to the process of epidermal wound healing and must be taken into account" [14, p.31]. This led to the expansion of the system to two reaction-diffusion equations, one for cell density and the other for the concentration of a specified mitosis activating or inhibiting chemical. These two equations then became the basis for the mathematical model of epidermal wound healing and demonstrate how mathematical

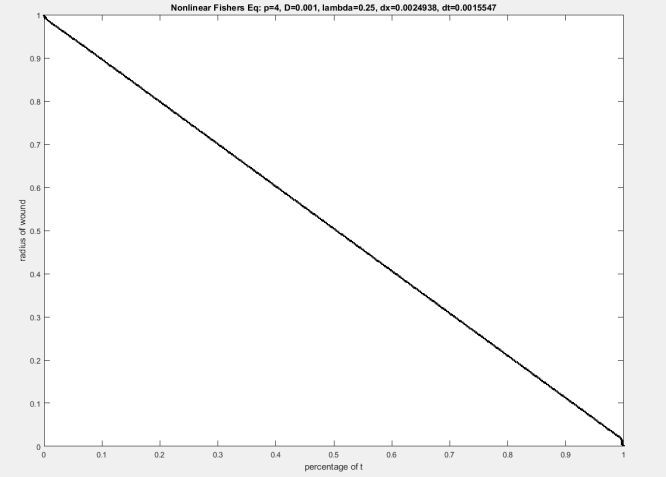

Figure 4: Time versus wound radius graph for the nonlinear diffusion case. The x-axis represents the percentage of the total time that the wound takes to heal and the y-axis represents the wound radius in non-dimensionalized coordinates.

modeling is relevant to epidermal wound healing beyond just simply predicting how long a specified wound will take to heal.

The idea of multiple reaction-diffusion equations was first described in Sherratt and Murray's initial paper [14], and then tweaked in many subsequent versions. In this improved model, a partial differential equation for chemical concentration, $c(\vec{x}, t)$ is added. The model needs to represent two different chemical regulators, one being an activator of mitosis and the other being an inhibitor of mitosis. Equations for both chemicals are necessary, to sufficiently model the biology of epidermal wound healing. Experimental evidence for the existence of both chemicals is extensive, with evidence for the inhibitor chemical coming from a study by Fremuth in 1984 [4] and evidence for the activator chemical coming from a study by Eisinger et al. in 1988 [3].

The following model comes from a 1991 paper by Sherratt and Murray [13] and represents the two governing reaction-diffusion equations for an improved mathematical model of epidermal wound healing. The two equations are

$$\boxed{\text{rate of change of cell density, } n} = \boxed{\text{cell migration}} + \boxed{\text{mitotic generation}} - \boxed{\text{natural loss}}, \quad (9)$$

$$\boxed{\text{rate of change of chemical concentration, } c} = \boxed{\text{diffusion of } c} + \boxed{\text{production of } c} - \boxed{\text{decay of chemical}}. \quad (10)$$

The cell migration and diffusion of the chemical terms are all modeled by simple Fickian diffusion. The cell migration term is modeled with linear diffusion because the authors found that "any nonlinearities [from the previous model] in the diffusive spread of epidermal cells are not fundamental to the healing process" [14, p. 32]. The diffusion of the chemical is

modeled by linear diffusion as well. Sherratt and Murray modeled the remaining terms by the following:

- $\boxed{\text{Natural loss}}$ - this term represents the natural decay and loss of epidermal skin cells. The loss of skin cells should be proportional to the cell density, so $\boxed{\text{natural loss}}=kn$ where k is a positive constant.

- $\boxed{\text{Mitotic generation}}$ - by Equation (1), without the presence of a biochemical regulator, the mitotic generation was of simple logistic growth with a positive growth parameter, s. Now that a chemical regulator has been introduced, the mitotic generation will be influenced by whether or not the presence of the specified chemical will activate or inhibit mitosis. To reflect this change mathematically, the authors introduced $s(c)$ as a function of the chemical concentration. Therefore the mitotic generation of the cells now depends on the interaction between the existing cells and the bioregulating chemical. This new form is $\boxed{\text{mitotic generation}}=s(c)\cdot n\cdot\left(2-\frac{n}{n_0}\right)$, where n_0 is again the unwounded cell density and $s(c)$ is a function of chemical concentration and thus depends on the activator chemical or the inhibitor chemical. For the activator chemical, $s(c)=k\cdot\frac{2c_m(h-\beta)c}{c_m^2+c^2}+\beta$ where h is a constant that corresponds to the max of $s(c)$, k is the coefficient of natural loss, c_m is a constant parameter that corresponds to the maximum level of chemical activation of mitosis, c_0 is the unwounded chemical concentration, and $\beta=\frac{c_0^2+c_m^2-2hc_0c_m}{(c_0-c_m)^2}$. For the inhibitor chemical, $s(c)=\frac{(h-1)c+hc_0}{2(h-1)c+c_0}\cdot k$.

  In the unwounded condition ($c=c_0$, $n=n_0$), the model requires that $s(c_0)=k$ where k is the linear mitotic rate. This is so that in the unwounded state, $\boxed{\text{mitotic generation}}-\boxed{\text{natural loss}}=kn\left(2-\frac{n}{n_0}\right)-kn=kn\left(1-\frac{n}{n_0}\right)$ which is in the form of the logistic growth as desired.

  For the activator chemical, we can show that $s(c_0)=k$. This calculation is shown in Appendix B.

  This is also true for the inhibitor chemical.

$$s(c_0)=\frac{(h-1)c_0+hc_0}{2(h-1)c_0+c_0}\cdot k=\frac{hc_0-c_0+hc_0}{2hc_0-2c_0+c_0}\cdot k=\frac{2hc_0-c_0}{2hc_0-c_0}\cdot k=k.$$

- $\boxed{\text{Decay of active chemical}}$ - this term follows from first order kinetics and thus can be modeled by $\boxed{\text{decay of active chemical}}=-\lambda c$ where λ is a positive constant.

- $\boxed{\text{Production of chemical by cells}}$ - this term also depends on whether the chemical activates or inhibits mitosis. The authors use the function $f(n)$, where $f(n)$ must satisfy two biologically relevant properties. First, with no cells there will be no production of c and thus $f(0)=0$. Also, in the unwounded condition there is no chemical in the first place, and thus $f(n_0)=\lambda c_0$ to cancel out the $\boxed{\text{decay of the active chemical}}$. For the activator chemical, the function $f(n)$ is modeled by

$$f(n)=\lambda c_0\cdot\frac{n}{n_0}\cdot\left(\frac{n_0^2+\alpha^2}{n^2+\alpha^2}\right),$$

and for the inhibitor chemical it is modeled by

$$f(n) = \frac{\lambda c_0}{n_0} \cdot n.$$

In both cases, it is clear that $f(0) = 0$ and $f(n_0) = \lambda c_0$ as required. The positive parameter α has also been introduced. The quantity α relates to the maximum rate of chemical production. This is because when $n = \alpha$, $f(n)$ will achieve its maximum. This can be shown using basic calculus. The derivative of f with respect to n is

$$f'(n) = \lambda c_o \frac{1}{n_0}\left(\frac{n_0^2+\alpha^2}{n^2+\alpha^2}\right) + \lambda c_0 \frac{n}{n_0}\left(-\frac{n_0^2+\alpha^2}{(n^2+\alpha^2)^2}\right)2n = \lambda c_o \frac{1}{n_0}\left(\frac{n_0^2+\alpha^2}{n^2+\alpha^2}\right)\left(1-\frac{2n^2}{n^2+\alpha^2}\right).$$

By setting the derivative equal to 0, then $\left(1-\frac{2n^2}{n^2+\alpha^2}\right) = 0$ and then $\alpha^2 - n^2 = 0$, and thus $\alpha = n$ is a critical value ($\alpha > 0$ and $n \geq 0$). By use of the second derivative test, it is clear that $(\alpha, f(\alpha))$ is a maximum. The second derivative of f with respect to n is

$$f''(n) = \lambda c_0 \frac{1}{n_0} \frac{2(n^3 - 3\alpha^2 n)(\alpha^2 + n_0^2)}{(\alpha^2+n^2)^3}.$$

This implies that

$$f''(\alpha) = \lambda c_0 \frac{1}{n_0} \frac{2(\alpha^3 - 3\alpha^2\alpha)(\alpha^2+n_0^2)}{(\alpha^2+\alpha^2)^3} = \lambda c_0 \frac{1}{n_0} \frac{2(-2\alpha^3)(\alpha^2+n_0^2)}{(2\alpha^2)^3} = \lambda c_0 \frac{-4}{n_0} \frac{(\alpha^3)(\alpha^2+n_0^2)}{(2\alpha^2)^3} < 0,$$

as $\lambda, c_0, n_0, \alpha > 0$. Therefore by the second derivative test $n = \alpha$ is indeed a maximum of $f(n)$.

Now by putting all of the terms together, the two reaction-diffusion equation full model is

$$\frac{\delta n}{\delta t} = D\nabla^2 n + s(c) \cdot n \cdot \left(2 - \frac{n}{n_0}\right) - kn, \tag{11}$$

$$\frac{\delta c}{\delta t} = D_c \nabla^2 c + f(n) - \lambda c, \tag{12}$$

with initial conditions $n(x,0) = 0, c(x,0) = 0$ for $x \in \Omega$ and boundary conditions $n(x,t) = n_0,\ c(x,t) = c_0$ for $x \in \partial\Omega$. This is a system of coupled nonlinear parabolic partial differential equations.

4.2 Non-dimensionalization of the model

Sherratt and Murray used standard techniques to non-dimensionalize the model. This means that they scaled the model in such a way that $c_0 = 1$ and $n_0 = 1$. Therefore, $c, n = 1$ in an unwounded setting and vary between 0 and 1 inside of a wound. They also standardized the length and timescale. To do this they introduced L as the length of the wound (or radius of the wound in a circular geometry), and a cell cycle timescale given by $\frac{1}{k}$. Non-dimensionalizing the model is a standard step in mathematical modeling and allows for easier mathematical and biological analysis. Sherratt and Murray used the scalings given by

$$n^* = \frac{n}{n_0},\ c^* = \frac{c}{c_0},\ x^* = \frac{x}{L},\ t^* = kt,\ D^* = \frac{D}{(kL^2)},\ \lambda^* = \frac{\lambda}{k},\ c_m^* = \frac{c_m}{c_0},\ \alpha^* = \frac{\alpha}{n_0},\ D_c^* = \frac{D_c}{(kL^2)}.$$

By applying the non-dimensionalization to the model (and also dropping the * for notational simplicity), Equations (11) and (12) become

$$\begin{aligned} \frac{\partial n}{\partial t} &= D\nabla^2 n + s(c)\cdot n\cdot(2-n) - n, \qquad (13)\\ \frac{\partial c}{\partial t} &= D_c\nabla^2 c + \lambda f(n) - \lambda c, \qquad (14) \end{aligned}$$

with initial conditions $n(x,0) = 0, c(x,0) = 0$ for $x \in \Omega$ and boundary conditions $n(x,t) = 1, c(x,t) = 1$ for $x \in \partial\Omega$.

For the activator chemical,

$$\begin{aligned} f(n) &= \frac{n(1+\alpha^2)}{n^2+\alpha^2},\\ s(c) &= \frac{2c_m(h-\beta)c}{c_m^2+c^2} + \beta, \end{aligned}$$

where $\beta = \frac{1+c_m^2-2hc_m}{(1-c_m)^2}$.
For the inhibitor chemical,

$$\begin{aligned} f(n) &= n,\\ s(c) &= \frac{(h-1)c+h}{2(h-1)c+1}. \end{aligned}$$

4.3 Numerical solution to the system

Sherratt and Murray numerically solved the non-dimensionalized system of partial differential equations (given by Equations (13) and (14)) through the method of lines for wounds with a circular (2-D) geometry. As this is a coupled and nonlinear system of two second order partial differential equations, no immediate direct solution technique exists, and thus the authors had to resort to numerical methods to find approximate solutions. They estimated the parameters by fitting their numerical solutions to data provided in the Brugal and Pelmont [1], Hennings et al. [6], Eisinger et al. [3], and Rytomaa and Kiviniemi [10] studies. These numerical solutions fit well with the experimental data and thus further indicate the importance of biochemical regulation in epidermal wound healing.

Using the method of lines and the parameter values given by Sherratt and Murray in [13] we can replicate their numerical solutions. To do this, we again use finite differences to discretize in time and space. We can then solve for the next time step and use a forward marching scheme to obtain numerical solutions. In the same method as before, this numerical system becomes

$$\begin{aligned} n_i^{j+1} &= D\frac{\Delta t}{(\Delta x)^2}\Big(n_{i-1}^j - 2n_i^j + n_{i+1}^j\Big) + \Delta t\cdot s(c_i^j)\cdot n_i^j\cdot(2-n_i^j) + n_i^j, \qquad (15)\\ c_i^{j+1} &= D_c\frac{\Delta t}{(\Delta x)^2}\Big(c_{i-1}^j - 2c_i^j + c_{i+1}^j\Big) + \Delta t\Big(\lambda f(n_i^{j+1}) - \lambda c_i^j\Big) + c_i^j, \qquad (16) \end{aligned}$$

where $\Delta x = \frac{1}{N}$ is the spatial step and Δt is the time step. We can again use a Forward Euler marching scheme to compute solution curves at each successive time step.

We have the initial condition $n(x,0) = 0, c(x,0) = 0$ inside the wound domain $[0,1)$. We also have the Dirichlet boundary condition of $n(1,t) = 1, c(1,t) = 1$, for all t. On the left hand boundary, we set a no flux boundary condition of $n_x(0,t) = 0, c_x(0,t) = 0$. These conditions, along with the iterative steps given by Equations (15) and (16) provide the full numerical scheme. The MATLAB code for this scheme is provided in Appendix A.5 (activator) and Appendix A.7 (inhibitor).

It is important to note here that we now have two CFL conditions, namely that

$$\begin{aligned} D\frac{\Delta t}{(\Delta x)^2} &\leq \frac{1}{2}, \\ D_c\frac{\Delta t}{(\Delta x)^2} &\leq \frac{1}{2}. \end{aligned}$$

Both of these must be satisfied in order for the numerical system to converge.

Figures 5, 6, 7, and 8 are the numerical solutions we found to the discretized system given by Equations (15) and (16). These solutions appear to be traveling waves that fit well with the experimental data. In both the activator and inhibitor case, the cell density has the characteristic 'lag then linear phase.' The solutions also show that the cell densities peak above the unwounded level of 1, an important feature shown in many biologically studies.

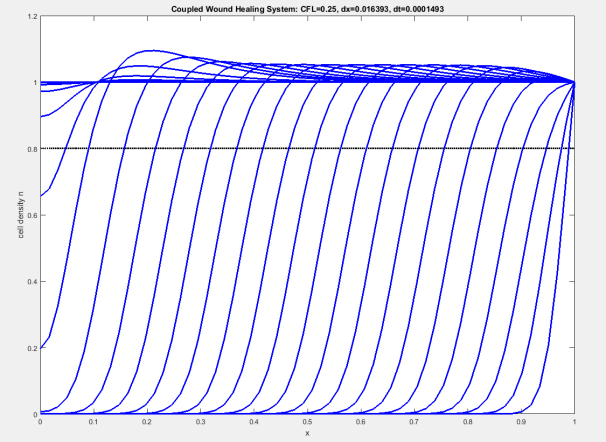

Figure 5: 1D Numerical solutions for cell density n in the activator case with parameter values $D = 5 \cdot 10^{-4}$, $D_c = 0.45$, $\lambda = 30, h = 10, \alpha = 0.1$, and $c_m = 40$.

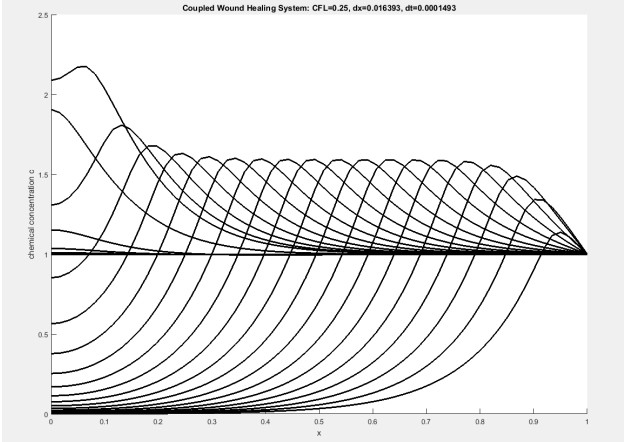

Figure 6: 1D Numerical solutions for chemical concentration c in the activator case with parameter values $D = 5 \cdot 10^{-4}$, $D_c = 0.45$, $\lambda = 30, h = 10, \alpha = 0.1$, and $c_m = 40$.

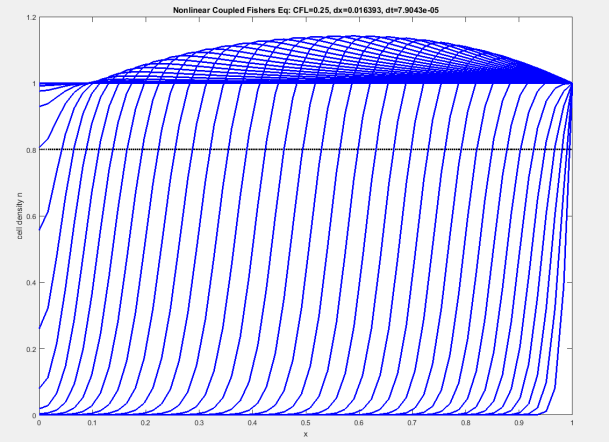

Figure 7: 1D Numerical solutions for cell density n in the inhibitor case with parameter values $D = 10^{-4},\ D_c = 0.85,\ \lambda = 5$, and $h = 10$.

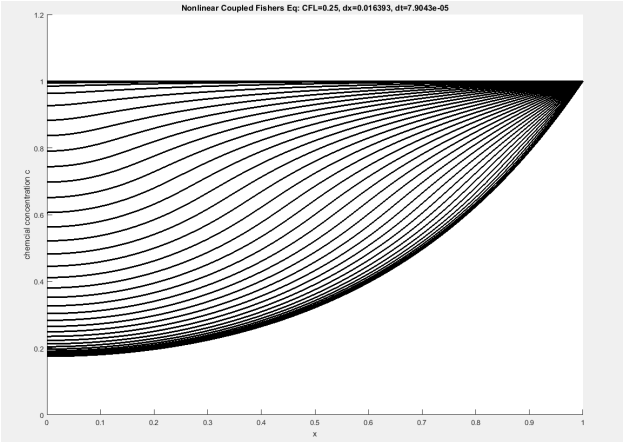

Figure 8: 1D Numerical solutions for chemical concentration c in the inhibitor case with parameter values $D = 10^{-4},\ D_c = 0.85,\ \lambda = 5$, and $h = 10$.

Figures 9 and 10 are the time versus wound radius plots using the same method as in the initial single reaction-diffusion equation model. The code used to make these graphs are given in Appendix A.6 (activator) and A.8 (inhibitor). As we can see from these plots, the model fits well with experimental data.

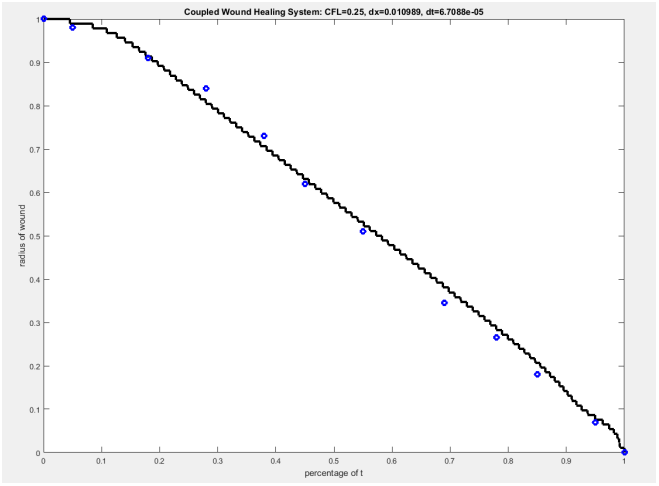

Figure 9: Time versus wound radius graph for the coupled activator case. The x-axis represents the percentage of the total time that the wound takes to heal and the y-axis represents the wound radius in non-dimensionalized coordinates. The blue circle data points represent experimentally found data from [16].

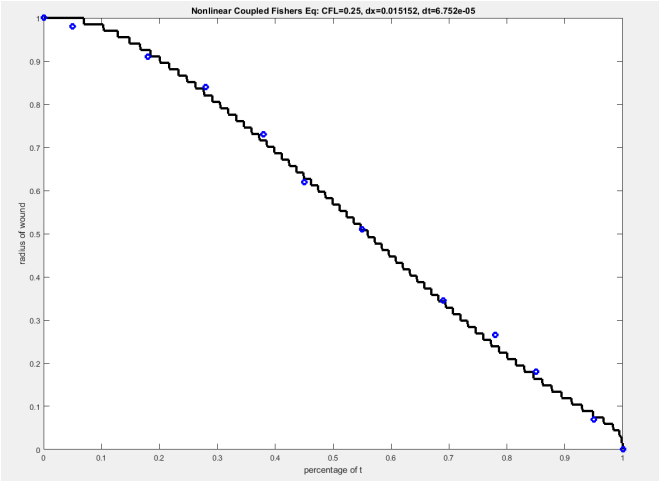

Figure 10: Time versus wound radius graph for the coupled inhibitor case. The x-axis represents the percentage of the total time that the wound takes to heal and the y-axis represents the wound radius in non-dimensionalized coordinates. The blue circle data points represent experimentally found data from [16].

4.4 Nova software numerical solutions to the system

In addition to numerical investigation of the problem, we can also implement the model in various mathematical modeling software. Using dedicated modelers allows us to easily tweak the model, and do rapid prototyping of any extensions. We can use the Nova computational modeler to implement the coupled Sherratt and Murray model of epidermal wound healing, seen in Figure 11. The modeler uses an agent-based model to solve the system in two dimensions.

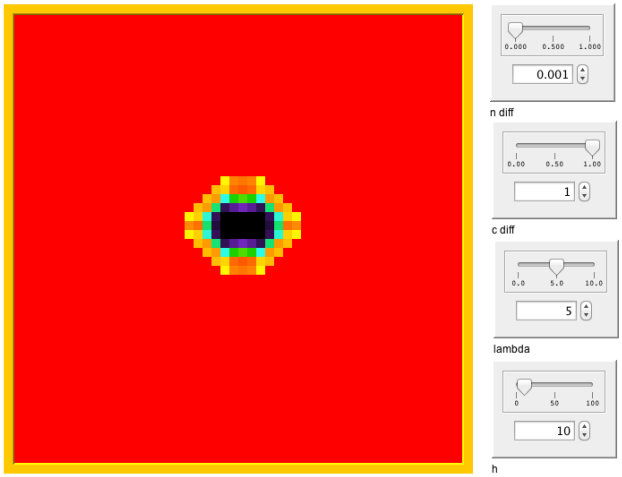

Figure 11: An epidermal wound in the middle of 'healing.' The red color represents unwounded epidermis whereas the black color represents the wounded area. The colors in-between represent the new epidermal cells diffusing into the wound, where different colors represent higher cell density (orange and yellow are higher then purple and blue). The sliders on the right allow the user to adjust model parameters.

5 Traveling wave solutions to a simplified ODE model

5.1 Method of characteristics

As seen in the numerical solutions to the coupled system, the solution curves look like potential traveling waves. A traveling wave is a distinct wave pattern that moves through space with a constant shape. Since we know that traveling waves exist for the Fisher equation and because the numerical solutions look like traveling waves, we can use the method of characteristics in order to look for these traveling wave solutions.

Initially, Sherratt and Murray considered two dimensional radially symmetric epidermal wounds. However, a one dimensional geometry is much more convenient to consider, as in a one dimensional geometry the model given by Equations (11) and (12) can be reduced into a two dimensional system of second order ordinary differential equations by the method of characteristics. This reduction is not possible in higher dimensions. Sherratt and Murray justified using this simplification based on the fact that large enough wounds of any shape are "one dimensional during most of the healing process" [13]. This is because they observed that for large wounds, small irregularities in the shape of the wound would be healed quickly because they have a large boundary and small wound space. Once these irregularities are gone, the wound can be approximated with an oval or circular shape with a decreasing radius.

Sherratt and Murray simplified the model via the method of characteristics [9]. They used characteristic variable z and made the transformation $z = x + at$ (where x is the spatial variable, t is time, and a is the wave speed). Using this simplification, the cell density and chemical concentration functions can be transformed into functions that only depend on the characteristic variable by letting $n(x,t) = N(z)$ and $c(x,t) = C(z)$. To transform the system into a system of ordinary differential equations, the authors first started with the non-dimensionalized form of the original model given again as

$$\frac{\partial n}{\partial t} = D\nabla^2 n + s(c)\cdot n\cdot(2-n) - n, \tag{17}$$

$$\frac{\partial c}{\partial t} = D_c\nabla^2 c + \lambda f(n) - \lambda c, \tag{18}$$

with initial conditions $n(x,0) = 0, c(x,0) = 0$ for $x \in \Omega$ and boundary conditions $n(x,t) = 1,\ c(x,t) = 1$ for $x \in \partial\Omega$.

Using the variable transformation described above, the partial derivative terms can all be transformed into derivatives in terms of z. The derivative transforms are given below, where the prime notation implies differentiation with respect to the characteristic variable z.

$$\begin{aligned}
\frac{\partial n(x,t)}{\partial t} &= \frac{dN(z)}{dz}\cdot\frac{\partial z(x,t)}{\partial t} = N'\cdot a = aN'.\\
D\nabla^2 n &= D\frac{\partial^2 n}{\partial x^2} = D\frac{d^2N(z)}{dz^2}\cdot\frac{\partial z(x,t)}{\partial x} = DN''.\\
D_c\nabla^2 c &= D_c\frac{\partial^2 c}{\partial x^2} = D_c\frac{d^2C(z)}{dz^2}\cdot\frac{\partial z(x,t)}{\partial x} = D_cC''.
\end{aligned}$$

Now by simply plugging the respective derivatives in, the model becomes a coupled system of ordinary differential equations given by

$$aN' = DN'' + s(C)\cdot N\cdot(2-N) - N, \tag{19}$$

$$aC' = D_cC'' + \lambda f(N) - \lambda C, \tag{20}$$

with biologically appropriate conditions of $N(-\infty) = C(-\infty) = 0,\ N(\infty) = C(\infty) = 1$, and $N'(\pm\infty) = C'(\pm\infty) = 0$.

Although the system has now been simplified to two ordinary differential equations, it is still a coupled and nonlinear system. Sherratt and Murray made some further simplifications to the model to look for analytic traveling wave solutions.

5.2 Simplification 1: Let $\lambda \to \infty$

This simplification represents the chemical concentration kinetics coming to a state of equilibrium. We make this simplification as it will reduce the system to a single second order ordinary differential equation, thus making the system easier to analyze. This is because as $\lambda \to \infty$, the terms not containing a λ in Equation (20) become negligible. So Equation (20) can be solved for C as shown below

$$\begin{aligned} 0 &= -aC' + D_c C'' + \lambda f(N) - \lambda C, \\ &= 0 + 0 + \lambda f(N) - \lambda C, \\ &= \lambda(f(N) - C). \end{aligned}$$

As $\lambda \neq 0$, this implies that $f(N) = C(z)$. We will also further simply the model by linearizing the $s(c)$ function. This linearization is given by $s(c) = \gamma c + 1 - \gamma$ where $\gamma = \frac{2(h-1)}{c_m - 2}$.

By rearranging terms from Equation (19) and plugging in $f(N) = C$, the system now be can represented by the single ordinary differential equation below

$$N'' = \frac{aN'}{D} - \frac{s(f(N)) \cdot N \cdot (2 - N) - N}{D}, \tag{21}$$

with boundary conditions $N(\infty) = 1,\ N(-\infty) = 0,\ N'(\pm\infty) = 0$ and where $N \geq 0$, as a negative cell density does not make biological sense.

We can now perform linear stability and asymptotic analysis on Equation (21). We can first change the system to two first order ordinary differential equations, by setting $N'(z) = M(z)$. The resulting system is given as

$$N' = M, \tag{22}$$

$$M' = \frac{aM - s(f(N)) \cdot N \cdot (2 - N) + N}{D}. \tag{23}$$

To find the singular values of the system we immediately have that $M = 0$. We also have that

$$\begin{aligned} 0 &= \frac{-s(f(N)) \cdot N \cdot (2 - N) + N}{D}, \\ &= -s(f(N)) \cdot N \cdot (2 - N) + N. \end{aligned}$$

This condition is satisfied when $N = 0$ and $N = 1$ as $f(0) = 0,\ s(1) = 1,\ f(1) = 1$. Therefore the equilibrium values are $(N, M) = (0, 0)$ and $(N, M) = (1, 0)$.

We have that the Jacobian J of the system given by Equations (22) and (23) is

$$J = \begin{bmatrix} 0 & 1 \\ \frac{-[s'(f(N)\cdot f'(N)\cdot N\cdot(2-N)+s(f(N))\cdot 1\cdot(2-N)-s(f(N))\cdot(N)-1]}{D} & \frac{a}{D} \end{bmatrix}$$

Therefore, at the the singular point $(0,0)$ the Jacobian evaluates to

$$J(0,0) = \begin{bmatrix} 0 & 1 \\ \frac{-[2s(0)-1]}{D} & \frac{a}{D} \end{bmatrix}$$

Using $\Lambda = \frac{1}{2}(T \pm \sqrt{T^2 - 4D_T})$ where T is the trace and D_T is the determinant (and we use Λ to represent the eigenvalues as λ has been defined earlier) we have that

$$\Lambda = \frac{1}{2}\Big[\frac{a}{D} \pm \sqrt{\Big(\frac{a}{D}\Big)^2 - 4\Big(\frac{2s(0)-1}{D}\Big)}\Big]. \tag{24}$$

To see where the phase plane changes at the bifurcation values we solve for $\sqrt{T^2 - 4D_T} = 0$ (also we require $a \geq 0$ as a physically represents a wave speed). Therefore we want to solve

$$\Big(\frac{a}{D}\Big)^2 - 4\Big(\frac{2s(0)-1}{D}\Big) = 0,$$

which implies that

$$\begin{aligned} & \tfrac{a^2}{D^2} && = 4\Big(\frac{2s(0)-1}{D}\Big), \\ \implies \quad & a^2 && = 4D\Big(2s(0)-1\Big), \\ \implies \quad & a && = 2\sqrt{\Big(D(2s(0)-1)\Big)}. \end{aligned}$$

Since $s(c) = \gamma c + 1 - \gamma$, we have that $s(0) = 1 - \gamma$. Thus the bifurcation value is

$$a^* = 2\sqrt{\Big(D(2(1-\gamma)-1)\Big)} = 2\sqrt{D(1-2\gamma)}.$$

At the singular point $(0,0)$, we have from Equation (24) that the system will have two positive real eigenvalues if $a > a^* = 2\sqrt{D(1-2\gamma)}$ and thus the singular point is an unstable node. If $a < a^* = 2\sqrt{D(1-2\gamma)}$ then we will have complex eigenvalues with positive real parts and the singular point is an unstable spiral. Using similar analysis as above we can classify the singular point at $(1,0)$ as a saddle point.

Similarly to Murray's analysis on the Fisher-Kolmogorov equation [9], we have that for $a > a^* = 2\sqrt{D(1-2\gamma)}$ there will be a heteroclinic orbit with $0 \leq N(z) \leq 1$ and $N'(z) \geq 0$ from the point $(0,0)$ to $(1,0)$. These are the traveling wave solutions to the system given by Equation (21). For all $a < 2\sqrt{D(1-2\gamma)}$ there are also traveling wave solutions but these are physically unrealistic as $N(z) < 0$ for some z as the heteroclinic orbit spirals around $(0,0)$.

Therefore, using this asymptotic analysis, we can conclude that there will be a traveling wave solution for every wave speed $a > a^* = 2\sqrt{D(1-2\gamma)}$ to the simplified system given by Equation (21). In Section 6, we will prove the same claim for the entire original system

given by Equations (13) and (14).

Sherratt and Murray numerically solved the system given by Equation (21). The shape of the solution curve for any order approximation looks approximately like the numerical solution found for the original system given in Equations (11) and (12). However, it fails to capture important features of the solution such as the part of the curve where the cell density is greater than 1 (in non-dimensionalized form). Therefore, the authors deemed that this simplification was not a reasonable approximation to make in order to model the full system of epidermal wound healing.

5.3 Simplification 2: Let $D = 0$

Sherratt and Murray justified this simplification because the biologically relevant D is already very small ($D \approx 10^{-4}$). This simplification biologically corresponds to the absence of cellular diffusion and implies that the only method of getting epidermal cells into the wounded region would be through mitosis. We make this simplification as it will reduce the cell density ordinary differential equation to a first order equation. Setting $D = 0$ in the system given by Equations (19) and (20) results in the simplified system given below

$$N' = \frac{s(C) \cdot N \cdot (2 - N)}{a} - \frac{N}{a}, \tag{25}$$

$$C'' = \frac{aC'}{D_c} - \frac{\lambda f(N)}{D_c} + \frac{\lambda C}{D_c}, \tag{26}$$

with boundary conditions $N(-\infty) = C(-\infty) = 0,\ N(\infty) = C(\infty) = 1,\ C(\pm\infty) = 0$, and with $N(z) \geq 0$ and $C(z) \geq 0$ for all z.

First, the authors solved this system numerically. Then they solved it analytically for the activator chemical through a perturbation method. This asymptotic analysis also produced a bound on the wave speed that compared favorably with previous results.

The solutions to Equations (25) and (26) compare well to the numerical solutions found for the original partial differential equation system given in Equations (11) and (12). Therefore, Sherratt and Murray deemed that setting $D = 0$ was a good and sensible approximation to make. This biologically implies that mitosis, rather than cellular diffusion, is the driving force behind epidermal wound healing and the regeneration of epidermal skin on the wound. This also represents a fantastic example of how a mathematical model can provide insight into a complex biological phenomena.

6 Traveling wave solutions to the full coupled PDE model

In a 2014 paper, mathematical biologists Haiyan Wang and Shillang Wu applied their previous work on non-cooperative reaction-diffusion systems to the epidermal wound healing model [18], [17]. This is the first time that traveling wave solutions to the full coupled Sherratt and Murray model for epidermal wound healing have been proven to exist, as results from the last section only dealt with simplified systems. Their general results are given in Appendix C. To understand their results, we begin with some terminology.

Consider the reaction-diffusion partial differential equation system given by

$$\frac{\partial A}{\partial t} = d_1 \nabla^2 A + g_1(A, B), \tag{27}$$

$$\frac{\partial B}{\partial t} = d_2 \nabla^2 B + g_2(A, B), \tag{28}$$

where g_1 and g_2 are differentiable functions of A and B. We call the system **cooperative** if

$$\frac{\partial g_1}{\partial B} \geq 0, \tag{29}$$

$$\frac{\partial g_2}{\partial A} \geq 0. \tag{30}$$

for $A, B > 0$. This terminology comes from population dynamics. If A and B are two populations that are in a symbiotic relationship (such as hippopotami and Oxpecker birds, clownfish and sea anemone, etc) then they will mutually benefit each other and the population of one will increase as the population of the other increases. Therefore, in these cooperative relationships, Equations (29) and (30) will be satisfied. If either Equation (29) or (30) is violated, then the system given by Equations (27) and (28) is called **non-cooperative**, such as in predator-prey models.

Wang and Wu began with the non-dimensionalized epidermal wound healing model for the activator case (with the linearized $s(c)$ function), given again below as

$$\frac{\partial n}{\partial t} = D\nabla^2 n + s(c) \cdot n \cdot (2 - n) - n, \tag{31}$$

$$\frac{\partial c}{\partial t} = D_c \nabla^2 c + \lambda f(n) - \lambda c, \tag{32}$$

with

$$f(n) = \frac{n(1 + \alpha^2)}{n^2 + \alpha^2},$$

$$s(c) = \gamma c + 1 - \gamma,$$

where $\gamma = \frac{2(h-1)}{c_m - 2}$.

This system is clearly non-cooperative, as $f(n)$ is not a monotone increasing function over the interval $0 \leq n \leq 1$. Using the notation above, we have that $g_1(n, c) = s(c) \cdot n \cdot (2 - n) - n$, $g_2(n, c) = \lambda f(n) - \lambda c$ and therefore

$$\frac{\partial g_1}{\partial c} = s'(c) \cdot n \cdot (2 - n) = \gamma \cdot n \cdot (2 - n), \tag{33}$$

$$\frac{\partial g_2}{\partial n} = \lambda f'(n) = \lambda \frac{(\alpha^2 - n^2)(1 + \alpha^2)}{(\alpha^2 + n^2)^2}. \tag{34}$$

Equation (33) is clearly nonnegative over $0 \leq n \leq 1$ as $\gamma > 0$. However, Equation (34) is negative when $n > \alpha = 0.1$. Therefore, in order to analyze this system, we will need Wang and Wu's results on non-cooperative reaction-diffusion systems [18]. With these results we can compare the non-cooperative system by an upper and lower bound cooperative system that will help us derive an analytic minimum limit for the traveling wave speed solutions as well as show the existence of traveling wave solutions.

Theorem 1. *(From [17]). Let D, D_c be positive constants and let $\gamma \in (0, \frac{1}{2}),\ \alpha \in (0,1)$,*

$$\frac{D_c}{D} < 2 + \frac{\lambda}{1-2\gamma}, \tag{35}$$

and

$$\frac{2\gamma f'(0)}{1-\gamma} = \begin{cases} 1 + \frac{1-2\gamma}{\lambda}, & D \geq D_c \\ \left(2 - \frac{D_c}{D}\right)\frac{1-2\gamma}{\lambda} + 1, & D \leq D_c \end{cases} \tag{36}$$

Then the system given by Equations (31) and (32) admits a physically relevant traveling wave solution for $a > a^*$ and does not admit a physically relevant traveling wave solution for $a < a^*$ where the minimum wave speed a^* is given by

$$a^* = 2\sqrt{(1-2\gamma)D},\ \Lambda_1 := \Lambda_1(a) = \frac{a - \sqrt{a^2 - 4D(1-2\gamma)}}{2D} > 0.$$

That is, the solution $(n(x,t), c(x,t))$ of the system satisfies

(i.) If the functions $(n(x,0), c(x,0)) \leq (k_1, k_2)$ are nonnegative continuous and have compact support, then

$$\lim_{t\to\infty} \sup_{|x|\geq at} (n(x,t), c(x,t)) = (0,0) \text{ for } a > a^*.$$

(ii.) If the functions $(n(x,0), c(x,0)) \leq (k_1, k_2)$ are nonnegative continuous and have compact support $n(x,0) \not\equiv 0$, then

$$(k_1^-, k_2^-) \leq \liminf_{t\to\infty} \inf_{|x|\leq at} (n(x,t), c(x,t)) \leq (k_1^+, k_2^+),\ \text{for } 0 < a < a^*.$$

(iii.) For each $a > a^*$ the system admits a traveling wave solution (N(z), C(z)) (under the variable transform $z = x + at$) such that $(0,0) \ll (N(z), C(z)) \leq (k_1^+, k_2^+), z \in \mathbb{R}$,

$$(k_1^-, k_2^-) \leq \lim_{z\to\infty} \inf(N(z), C(z)) \leq \lim_{z\to\infty} \sup(N(z), C(z)) \leq (k_1^+, k_2^+),$$

and

$$\lim_{z\to-\infty} (N(z), C(z)) e^{-\Lambda(a)z} = v_{\Lambda_1}.$$

(iv.) For $a = a^*$ the system admits a nonconstant traveling wave solution $(N(z), C(z))$ such that $(0,0) \leq (N(z), C(z)) \leq (k_1^+, k_2^+), z \in \mathbb{R}$.

(v.) For $0 < a < a^*$ the system does not admit a traveling wave solution $(N(z), C(z))$ with $\lim_{z\to\infty} \inf(N(z), C(z)) \gg (0,0)$ and $(N(-\infty), C(-\infty)) = 0$.

In order prove Theorem 1 we will apply the conditions of H_1, H_2, and H_3 and the results of Theorem 2 (see Appendix C). First, we must show that the epidermal wound healing system given by Equations (31) and (32) satisfies the conditions of H_1.

6.1 Verifying H_1

The system has two equilibrium values, (0,0) and (1,1). The equilibrium values will occur when the reaction functions are simultaneously equal to 0 which means that

$$\begin{aligned} 0 &= s(c) \cdot n \cdot (2-n) - n, \quad (37) \\ 0 &= \lambda(f(n) - c). \quad (38) \end{aligned}$$

At (0,0) we have that

$$\begin{aligned} 0 &= (1-\gamma) \cdot 0 \cdot (2-0) - 0 = 0, \ \checkmark \\ 0 &= \lambda(0-0) = 0, \ \checkmark \end{aligned}$$

and at (1,1) we have that

$$\begin{aligned} 0 &= 1 \cdot 1 \cdot (2-1) - 1 = 0, \ \checkmark \\ 0 &= \lambda(1-1) = 0. \ \checkmark \end{aligned}$$

There are also no other equilibrium between these values because from Equation (38) we have that at any proposed equilibrium values, $f(n) = c$. By plugging this into Equation (37) we have that $s(f(n)) \cdot n \cdot (2-n) - n = 0$. At any nonzero equilibrium, this implies that

$$(f(n)\gamma + 1 + \gamma) \cdot n \cdot (2-n) - n = 0,$$

and thus that

$$\begin{aligned} f(n) &= \frac{\frac{1}{2-n} + \gamma - 1}{\gamma}, \\ f(n) &= c, \end{aligned}$$

which is only satisfied at $(n, c) = (1, 1)$.

Now, we can find the two cooperative systems that bound our system. Since the system given by Equations (31) and (32) is non-cooperative only because of the $f(n)$ function, this will involve finding the appropriate $f^{\pm}$ functions.

Recall from Section 4.1 that $f(n) = \frac{n(1+\alpha^2)}{n^2+\alpha^2}$ and that the maximum of this function (here non-dimensionalized) occurs when $n = \alpha$. Therefore we will define

$$f^+(n) = \begin{cases} f(n), & 0 \le n \le \alpha \\ f(\alpha), & n \ge \alpha \end{cases}$$

which is clearly monotone increasing as f^+ increases from $[0, \alpha]$ and then becomes constant. The corresponding cooperative system is

$$\begin{aligned} \frac{\partial n}{\partial t} &= D\nabla^2 n + s(c) \cdot n \cdot (2-n) - n, \quad (39) \\ \frac{\partial c}{\partial t} &= D_c \nabla^2 c + \lambda f^+(n) - \lambda c. \quad (40) \end{aligned}$$

Similarly to the analysis above, the system given by Equations (39) and (40) will have two equilibrium values. Clearly $(0, 0)$ is still an equilibrium value and we have that at the nonzero equilibrium (k_1^+, k_2^+) that

$$\begin{aligned} f^+(k_1^+) &= \frac{\frac{1}{2-k_1^+} + \gamma - 1}{\gamma}, \\ f^+(k_1^+) &= k_2^+. \end{aligned}$$

Given the Equations above and the definition of f^+, solving for (k_1^+, k_2^+) is straightforward and we have that

$$\begin{aligned} k_1^+ &= 2 - \frac{1}{1 + (\frac{1+\alpha^2}{2\alpha} - 1)\gamma} > 1 > \alpha, \\ k_2^+ &= \frac{1+\alpha^2}{2\alpha} > 1. \end{aligned}$$

Now we must define the other appropriate cooperative system that bounds the epidermal wound healing system below. Since f is continuous and monotone increasing over the interval $[0, \alpha]$, there must exist an $f_0 \in (0, \alpha]$ such that $f(f_0) < \min\{1, f(k_1^+)\}$. Thus we will define

$$f^-(n) = \begin{cases} f(n), & 0 \le n \le f_0 \\ f(f_0), & n > f_0 \end{cases}$$

Here we can note that from the definitions of the cooperative systems, it is clear for $n \in (0, k_1^+]$ that

$$0 < f^-(n) \le f(n) \le f^+(n) \le f'(0)n = \frac{n(\alpha^2+1)}{\alpha^2}, \tag{41}$$

and that $f^-(n) < 1$ for biologically relevant $n \ge 0$ (recall that we calculated $f'(n)$ in Section 4.1).

The corresponding cooperative system is

$$\frac{\partial n}{\partial t} = D\nabla^2 n + s(c) \cdot n \cdot (2 - n) - n, \tag{42}$$

$$\frac{\partial c}{\partial t} = D_c \nabla^2 c + \lambda f^-(n) - \lambda c. \tag{43}$$

Similarly to the analysis above, the system given by Equations (42) and (43) will have two equilibrium values. Clearly $(0, 0)$ is still an equilibrium value and we have that at the nonzero equilibrium (k_1^-, k_2^-) that

$$\begin{aligned} f^-(k_1^-) &= \frac{\frac{1}{2-k_1^-} + \gamma - 1}{\gamma}, \\ f^-(k_1^-) &= k_2^-. \end{aligned}$$

Given the Equations above and the definition of f^-, solving for k_1^- is straightforward and we have that

$$k_1^- = 2 - \frac{1}{1 + (f(f_0) - 1)\gamma} < 1 \text{ as } f(f_0) < 1,$$

and that $0 < k_2^- = f^-(k_1^-) < 1$. From the definitions of the equilibrium values it is clear that

$$(0, 0) \ll (k_1^-, k_2^-) \le (1, 1) \le (k_1^+, k_2^+).$$

Since the cooperative systems given by Equations (39), (40) and (42), (43) are piecewise bounded and differentiable, then the Maximum Principle implies that $0 \le u(x, t) \le k^+$ for $x \in \mathbb{R}, t > 0$.

Finally, to finish checking the conditions of H_1, we need to show that the two systems given by Equations (39), (40) and (42), (43) have the same Jacobian matrix at $(n, c) = (0, 0)$. This is clearly the case as $f^+(n) = f^-(n) = f(n)$ in a neighborhood of 0 (specifically over the interval $[0, f_0]$) and thus the derivative of all three functions at 0 will be equal.

6.2 Verifying H_2

Therefore, we have that the conditions of H_1 are satisfied for the Sherratt and Murray epidermal wound healing model. Now we need to check the conditions of H_2. To begin, we need to find the linearization of the Sherratt and Murray system given by Equations (31) and (32) at the origin. We have that the reaction functions g_1 and g_2 are

$$\begin{aligned} g_1(n,c) &= s(c)\cdot n\cdot(2-n)-n = (\gamma c+1-\gamma)\cdot n\cdot(2-n)-n, \\ g_2(n,c) &= \lambda f(n)-\lambda c. \end{aligned}$$

The relevant partial derivatives of the reaction functions g_1 and g_2 are

$$\begin{aligned} \frac{\partial g_1}{\partial n} &= (\gamma c+1-\gamma)(2-n)-s(c)\cdot n-1, \\ \frac{\partial g_1}{\partial c} &= \gamma\cdot n\cdot(2-n)-n, \\ \frac{\partial g_2}{\partial n} &= \lambda f'(n), \\ \frac{\partial g_2}{\partial c} &= -\lambda. \end{aligned}$$

Evaluated at the origin we have that

$$\begin{aligned} \frac{\partial g_1(0,0)}{\partial n} &= (\gamma c+1-\gamma)(2-n)-s(c)\cdot n-1 = (1-\gamma)(2)-1 = 1-2\gamma, \\ \frac{\partial g_1(0,0)}{\partial c} &= \gamma\cdot n\cdot(2-n)-n = 0, \\ \frac{\partial g_2(0,0)}{\partial n} &= \lambda f'(n) = \lambda f'(0), \\ \frac{\partial g_2(0,0)}{\partial c} &= -\lambda. \end{aligned}$$

Therefore the linearization of Equations (31) and (32) at the origin is

$$\frac{\partial n}{\partial t} = D\nabla^2 n + s(c)\cdot n\cdot(2-n)-n, \tag{44}$$

$$\frac{\partial c}{\partial t} = D_c\nabla^2 c + \lambda f(n)-\lambda c. \tag{45}$$

Now we can build the coefficients of the characteristic equation (A_Λ) matrix where $A_\Lambda = \text{diag}(d_i\Lambda^2) + g'(0)$ and

$$\begin{aligned} g'(0) &= \begin{bmatrix} \frac{\partial g_1(0,0)}{\partial n} & \frac{\partial g_1(0,0)}{\partial c} \\ \frac{\partial g_2(0,0)}{\partial n} & \frac{\partial g_2(0,0)}{\partial c} \end{bmatrix} \\ &= \begin{bmatrix} 1-2\gamma & 0 \\ \lambda f'(0) & -\lambda \end{bmatrix} \end{aligned}$$

Thus we have that,

$$A_\Lambda = \begin{bmatrix} D\Lambda^2+1-2\gamma & 0 \\ \lambda f'(0) & D_c\Lambda^2-\lambda \end{bmatrix}$$

From inspection we can find two eigenvalues, namely

$$\begin{bmatrix} D\Lambda^2+1-2\gamma & 0 \\ \lambda f'(0) & D_c^2\Lambda-\lambda \end{bmatrix} \begin{bmatrix} 1 \\ 0 \end{bmatrix} = (D\Lambda^2+1-2\gamma)\begin{bmatrix} 1 \\ 0 \end{bmatrix}$$

and

$$\begin{bmatrix} D\Lambda^2+1-2\gamma & 0 \\ \lambda f'(0) & D_c^2\Lambda-\lambda \end{bmatrix} \begin{bmatrix} 0 \\ 1 \end{bmatrix} = (D_c\Lambda^2-\lambda) \begin{bmatrix} 0 \\ 1 \end{bmatrix}$$

As Wang and Wu point out, $D\Lambda^2+1-2\gamma$ is the principal eigenvalue of A_λ [17]. We can define

$$\Phi(\Lambda) = \frac{D\Lambda^2+1-2\gamma}{\Lambda}, \tag{46}$$

and then

$$\Phi'(\Lambda) = \frac{(\Lambda)(2D\Lambda^2)-(D\Lambda^2+1-2\gamma)(1)}{\Lambda^2} = \frac{D\Lambda^2-1+2\gamma}{\Lambda^2}. \tag{47}$$

To find the critical values of $\Phi(\Lambda)$ we set $\frac{D\Lambda^2-1+2\gamma}{\Lambda^2}=0$. This implies that $D\Lambda^2-1+2\gamma=0$ and thus that $\Lambda=\sqrt{\frac{1-2\gamma}{D}}$ as we choose $\Lambda>0$.

We can show that this critical value is a minimum as

$$\begin{aligned} \Phi''(\Lambda) &= \frac{(\Lambda^2)(2D\Lambda)-(D\Lambda^2-1+2\gamma)(2\Lambda)}{\Lambda^4}, \\ &= \frac{2D\Lambda^3-2D\Lambda^3+2\Lambda-4\Lambda\gamma}{\Lambda^4}, \\ &= \frac{2\Lambda-4\Lambda\gamma}{\Lambda^4}, \\ &= \frac{2\Lambda(1-2\gamma)}{\Lambda^4}, \end{aligned}$$

and thus

$$\Phi''\Big(\sqrt{\frac{1-2\gamma}{D}}\Big) = \frac{2\sqrt{\frac{1-2\gamma}{D}}(1-2\gamma)}{\sqrt{\frac{1-2\gamma}{D}}^4},$$

which is positive as $\sqrt{\frac{1-2\gamma}{D}}>0$ and $\gamma\in(0,\frac{1}{2})$. Thus we have that $\Phi''(\Lambda)>0$ and therefore $\Phi(\Lambda)$ achieves a minimum at $\Lambda=\sqrt{\frac{1-2\gamma}{D}}$ by the second derivative test.

This minimum value of $\Phi(\Lambda)$ is

$$\begin{aligned} \Phi\Big(\sqrt{\frac{1-2\gamma}{D}}\Big) &= \frac{D\Big(\sqrt{\frac{1-2\gamma}{D}}\Big)^2+1-2\gamma}{\sqrt{\frac{1-2\gamma}{D}}}, \\ &= \frac{1-2\gamma+1-2\gamma}{\sqrt{\frac{1-2\gamma}{D}}}, \\ &= \frac{2(1-2\gamma)D^{1/2}}{(1-2\gamma)^{1/2}}, \\ &= 2\sqrt{(1-2\gamma)D}, \\ &= a^*. \end{aligned}$$

Therefore,

$$\Lambda_1(a) = \frac{a-\sqrt{a^2-4D(1-2\gamma)}}{2D}, \tag{48}$$

has a bifurcation value at $a^* = 2\sqrt{(1-2\gamma)D}$ which is the critical minimum wave speed for the wound healing system.

Now, we let $\Lambda^* = \sqrt{\frac{1-2\gamma}{D}}$. For each $0 \leq \Lambda \leq \Lambda^*$, the positive eigenvector of A_Λ corresponding to the principle eigenvalue $D\Lambda^2 + 1 - 2\gamma$ is

$$\begin{pmatrix} v_{\Lambda,1} \\ v_{\Lambda,2} \end{pmatrix} = v_\Lambda = \begin{pmatrix} v_\Lambda^{(1)} \\ v_\Lambda^{(2)} \end{pmatrix} = \begin{pmatrix} (D-D_c)\Lambda^2 + 1 - 2\gamma + \lambda \\ \lambda f'(0) \end{pmatrix}$$

To verify that $A_\Lambda v_\Lambda = (D\Lambda^2 + 1 - 2\gamma)v_\Lambda$ we have that

$$\begin{bmatrix} D\Lambda^2 + 1 - 2\gamma & 0 \\ \lambda f'(0) & D_c\Lambda^2 - \lambda \end{bmatrix} \begin{pmatrix} (D-D_c)\Lambda^2 + 1 - 2\gamma + \lambda \\ \lambda f'(0) \end{pmatrix}$$

$$= (D\Lambda^2 + 1 - 2\gamma) \begin{pmatrix} (D-D_c)\Lambda^2 + 1 - 2\gamma + \lambda \\ \lambda f'(0) \end{pmatrix}$$

Therefore, we just need to show that

$$\begin{aligned} &(D\Lambda^2 + 1 - 2\gamma)((D-D_c)\Lambda^2 + 1 - 2\gamma + \lambda) + (0)(\lambda f'(0)), \\ &= (D\Lambda^2 + 1 - 2\gamma)((D-D_c)\Lambda^2 + 1 - 2\gamma + \lambda), \ \checkmark \end{aligned}$$

and

$$\begin{aligned} &(\lambda f'(0))((D-D_c)\Lambda^2 + 1 - 2\gamma + \lambda) + (D_c\Lambda^2 - \lambda)(\lambda f'(0)), \\ &= (\lambda f'(0))((D-D_c)\Lambda^2 + 1 - 2\gamma + \lambda + D_c\Lambda^2 - \lambda), \\ &= (\lambda f'(0))(D\Lambda^2 - D_c\Lambda^2 + 1 - 2\gamma + \lambda + D_c\Lambda^2 - \lambda), \\ &= (D\Lambda^2 + 1 - 2\gamma)(\lambda f'(0)). \ \checkmark \end{aligned}$$

Further, we have that $v_\Lambda^1, v_\Lambda^2 > 0$ as $\gamma \in (0, \frac{1}{2}), \lambda > 0$, and $f'(0) > 0$. Since v_λ is clearly continuous for $\Lambda > 0$, then we have that the conditions of H_2 are satisfied by the epidermal wound healing system.

6.3 Verifying H_3

Now we must verify H_3. First, for any $n \in \mathbb{Z}^+, \eta_1, .., \eta_n > 0$ and $\Lambda_1, ..., \Lambda_n \in [0, \Lambda^*]$, we let

$$(z_1, z_2) := (\eta_1 v_{\Lambda 1}^1 + ... + \eta_n v_{\Lambda n}^1, \eta_1 v_{\Lambda 1}^2 + ... + \eta_n v_{\Lambda n}^2 \gg (0,0).$$

To show that H_3 is satisfied by the system, we simply need that the following inequality holds

$$g^+(\eta v_\Lambda) \leq \eta g'(0) v_\Lambda.$$

In terms of the epidermal wound healing system, this means that

$$\begin{aligned} (\gamma z_2 + 1 + \gamma) z_1(2 - z_1) - z_1 &\leq (1 - 2\gamma) z_1, & (49) \\ b f^+(z_1) - b z_2 &\leq b f'(0) z_1 - b z_2. & (50) \end{aligned}$$

Recall from Equation (41) that $f^+(n) \leq f'(0)n$, and thus we immediately have that Equation (50) holds. Equation (49) is equivalent to

$$2\gamma z_1 z_2 - \gamma z_1^2 z_2 + 2z_1 - z_1^2 - 2\gamma z_1 + \gamma z_1^2 - z_1 \leq z_1 - 2z_1\gamma,$$

which implies that

$$\begin{aligned} 2\gamma z_1 z_2 - \gamma z_1^2 z_2 &\leq z_1^2 - \gamma z_1, \\ (2\gamma - \gamma z_1) z_2 &\leq z_1(1-\gamma), \\ (2 - z_1)\gamma &\leq \frac{z_1}{z_2}(1-\gamma), \\ \frac{(2-z_1)\gamma}{(1-\gamma)} &\leq \frac{z_1}{z_2}. \end{aligned}$$

From Equation (36) we have that for any $\Lambda \in [0, \Lambda^*]$,

$$\frac{z_1}{z_2} \geq \begin{cases} \left(1 + \frac{1-2\gamma}{\lambda}\right)/f'(0) & , \text{ if } D \geq D_c \\ \left[\left(2 - \frac{D}{D_c}\right)\frac{1-2\gamma}{\lambda} + 1\right]/f'(0) & , \text{ if } D < D_c \end{cases} \tag{51}$$

Since $f'(0) = 1 + \frac{1}{\alpha^2} > 1$, from Equation (51) we can see that $\frac{(2-z_1)\gamma}{(1-\gamma)} \leq \frac{z_1}{z_2}$ is satisfied and thus Equation (49) is satisfied.

Therefore H_1, H_2 and H_3 are satisfied by the Sherratt and Murray epidermal wound healing system given by Equations (31) and (32). This means that we can apply Theorem 2 to the system and then we have that Theorem 1 holds for parameter values that satisfy Equations (35) and (36). Thus we have proven that for every wave speed $a > a^*$ there will be a unique traveling wave solution to the epidermal wound healing system. As Sherratt and Murray only derive traveling wave solutions for simplified systems and use perturbative approximations [13], this is the first time that analytic solutions with no approximations to the entire system have been shown to exist.

7 Clinical implications of the model

7.1 Varying wound geometry

Previously in their investigation, Sherratt and Murray only considered circular epidermal wounds. However, once a working model that fit well with experimental data was created, Sherratt and Murray were able to "make theoretical predictions, by doing 'mathematical experiments' [with regard to wound shape] [12]". The authors were able to quantifiably change the shape of a wound by varying the value of α (parameter that corresponds to the maximum rate of chemical production) over the interval $[-1, 1]$. They found different shapes for different α values which are detailed below. Figure 12 shows the different shapes given by different α values. The functional form of the wound shapes they considered is

$$f_{shape}(x;\alpha) = \frac{1}{2}\left(1 + \frac{1}{\alpha}\right) - \text{sign}(\alpha)\left[\frac{1}{2}\left(1 + \frac{1}{\alpha^2}\right) - \left(x + \frac{1}{2\alpha} - \frac{1}{2}\right)^2\right]^{1/2}.$$

- $\alpha = -1$ implies the wound shape is a cusp.
- $-1 < \alpha < 0$ implies the wound shape is a cusped diamond.
- $\alpha = 0$ implies the wound shape is a diamond.
- $0 < \alpha < 1$ implies the wound shape is more ovate.

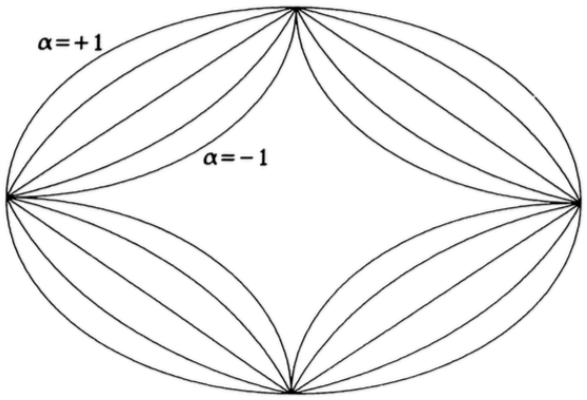

Figure 12: Varying wound shapes, parameterized by $\alpha \in [-1, 1]$. Wound shapes are not drawn to scale, as each shape has the same area regardless of α value (Taken from [11]).

- $\alpha = 1$ implies the wound shape is an ellipse.

Sherratt and Murray numerically solved the coupled non-dimensionalized partial differential equation system given by Equations (13) and (14) for a selection of α values between -1 and 1. They solved the system for both the activator chemical mechanism and the inhibitor chemical mechanism. Figure 13 shows what they found, where healing time is expressed as a percentage of total healing time found before.

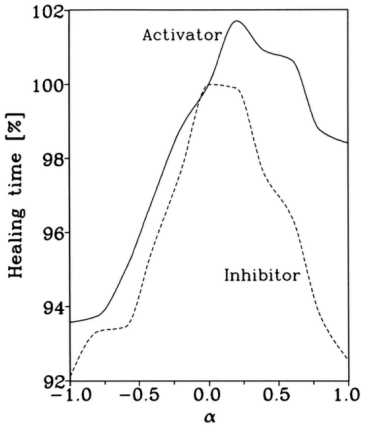

Figure 13: Wound shape healing time, parameterized by $\alpha \in [-1, 1]$. Healing time is expressed as a percentage of total healing time found when α was not varied (Taken from [11]).

Intuitively, it is not clear for example why the inhibitor mechanism would heal a wound almost 6 percentage points faster than the activator mechanism for $\alpha = 1$. Sherratt and Murray were able to justify this by Figure 14. This Figure demonstrates how the shape of the wound changes based on whether the activator/inhibitor mechanism is in play. When $\alpha = 1$, the inhibitor chemical mechanism flattens the wound much faster than the activator mechanism. This causes the overall wounded area to decrease faster and thus the overall healing time will decrease as well.

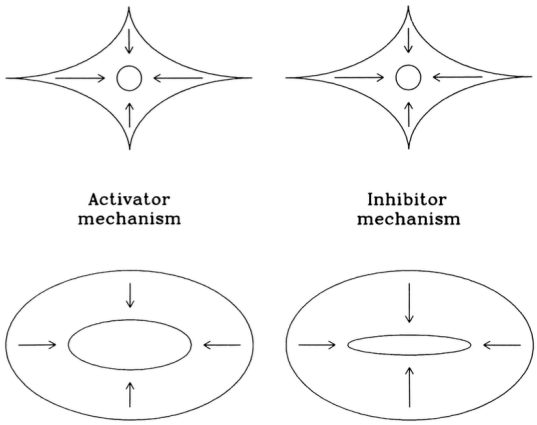

Figure 14: Wound shape as healing progresses, parameterized by $\alpha \in [-1, 1]$. The shapes demonstrate how the activator mechanism and inhibitor mechanism heal wounds differently (Taken from [11]).

We can use the Nova software to compare the effect of wound shape on total healing time. Figure 15 shows two epidermal wounds with similar surface area healing at different speeds, which confirm Sherratt and Murray's results given by Figure 13.

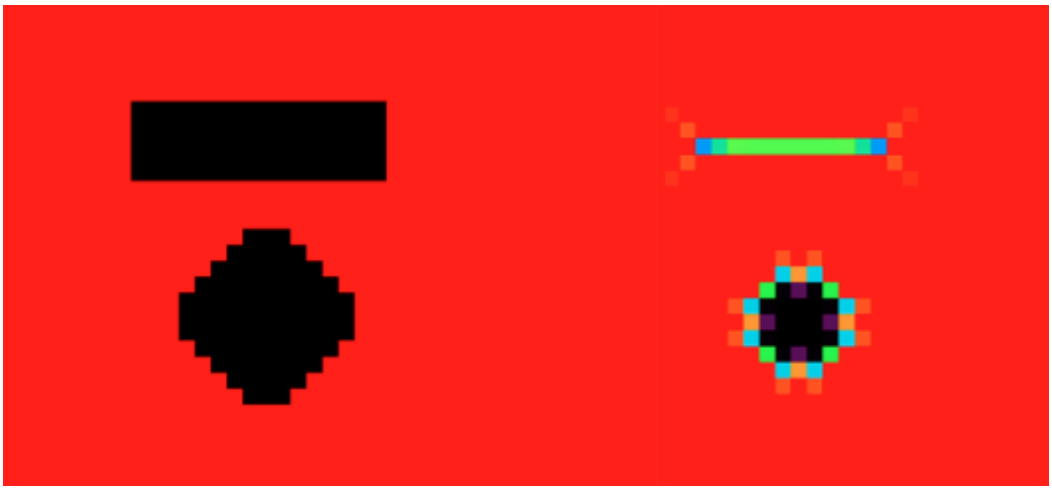

Figure 15: Two epidermal wounds under the inhibitor mechanism. The wound on top corresponds to a higher α value. The Figure shows the wound at $t = 0$ and then at a later time where the wound with a higher α value is almost completely done healing. This helps to show how different α values can have an effect on total wound healing time.

Sherratt and Murray's 'mathematical experimentation' with wound shape represents one of the advantages of mathematical modeling. These mathematical projections could be tested and verified via further biological research. They provide real world clinical implications, simply by playing with one parameter in the model.

7.2 Topical application of mitosis regulating chemicals

Sherratt and Murray also used their mathematical model to investigate the effect of external additions of mitosis regulating chemicals to the wounded area. They found that a one time burst of chemical (either the activator or inhibitor) had little to no effect on healing time. However, when the chemical was applied over an extended period of time, it had a much larger effect on the healing time. Figure 16 shows their results when they numerically solved models in which mitosis regulating chemicals were mathematically topically applied to the wound.

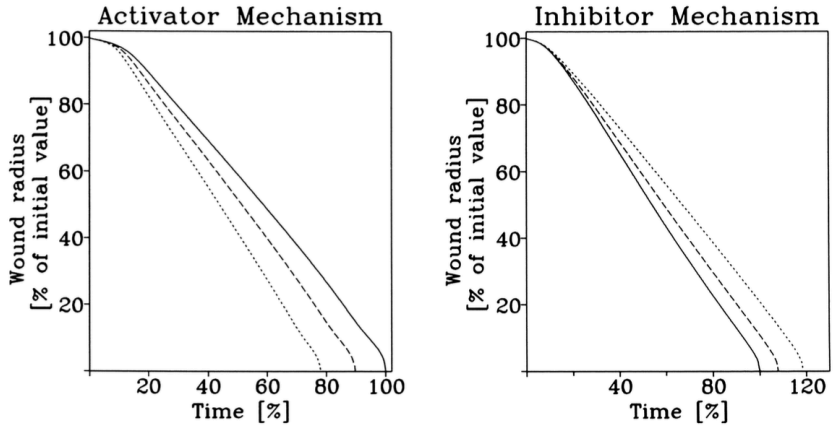

Figure 16: The model prediction of the effects of a constant gradual release of mitosis-regulating chemical onto healing epidermal wound. The solid curves denote the healing profile for a control wound with either auto activation or auto inhibition of mitosis, and time is expressed as a percentage of the total healing time in these cases. The dashed curves denote the healing profile when chemical is added to the wounded area throughout healing. In each case, we show the results for two different rates of chemical release. which are $\frac{c_0}{5}$ (- - -) and $\frac{c_0}{20}$ $(\cdots)$ per hour in the activator case and $\frac{c_0}{50}$ (- - -) and $\frac{c_0}{2}$ $(\cdots)$ per hour in the inhibitor case. Here c_0 is the concentration of regulatory chemical in unwounded epidermis. (Taken from [11]).

Figure 16 details how the topical application of the activator of mitosis increased healing time whereas the topical application of an inhibitor of mitosis decreased healing time. These model predictions could be biologically tested and are certainly medically relevant and applicable results, as they could indicate a way to speed up the healing process of epidermal wounds. Furthermore, Sherratt and Murray's model gives a relation between change in healing time and the ratio of amount of chemical release per unit of time and the concentration of the chemical in the unwounded skin. This could be implemented as a new way to calculate chemical concentration in the skin. These projections represent another 'mathematical experiment' that provides real world clinical implications that can be tested and verified via further biological research.

8 Conclusion

The mathematical modeling of epidermal wound healing demonstrates how applicable biomathematical models can be used to provide insight into complex (and not fully understood) systems. Not only can the introduced models be used to calculate things such as wound healing time, but they also are used to analyze which biological factors influence wound healing the

most. Furthermore, they are even used to conduct 'mathematical experiments', which could have real world medical implications.

The mathematical models presented generally increase chronologically in their mathematical and biological sophistication. We began with a single reaction-diffusion model, which was shown to be insufficient to model epidermal wound healing. This led to the creation of a two reaction-diffusion equation model. It was with this model that we then performed analysis on and numerically solved using the method of lines. It was also demonstrated that there exists rigorous traveling wave solutions to this reaction-diffusion system, which is a very recent result.

The level of sophistication of the models is also a product of new computing and modeling technology that has greatly advanced and elevated the mathematical biology field. This has led, and will continue to lead, to new biomathematical research and understanding of the process of epidermal wound healing. In this case, the Nova computational modeling software was a great tool to help us visualize the mathematics of epidermal wound healing.

Overall, since epidermal wound healing is a very common and pervasive affliction that is not fully understood, it provides rich opportunities for new models and new research in both biology and mathematical biology.

Acknowledgements

I would very much like to thank my advisor, Professor Ron Buckmire, for his help, ideas, and for the numerous times reading through my paper. I would also like to thank the Occidental College Mathematics Department as well as many alumni that have helped and inspired me throughout my time at Oxy including Emily Heath, Brandon Martelli, Mary Kemp, Alex Barylskiy, Jonathan Fernandez, Andrew Featherston, Sirena Van Epp and many more. Finally, I would like to thank Professor Viktor Grigoryan for all of his help and for the introduction to mathematical modeling, mathematical biology, and partial differential equations.

References

[1] Brugal, G., and J. Pelmont. "Existence of two chalone-like substances in intestinal extract from the adult newt, inhibiting embryonic intestinal cell proliferation." *Cell Proliferation* 8.2 (1975): 171-187.

[2] Dale, Paul D., Philip K. Maini, and Jonathan A. Sherratt. "Mathematical modeling of corneal epithelial wound healing." *Mathematical biosciences* 124.2 (1994): 127-147.

[3] Eisinger, M., et al. "Growth regulation of skin cells by epidermal cell-derived factors: implications for wound healing." *Proceedings of the National Academy of Sciences* 85.6 (1988): 1937-1941.

[4] Fremuth, Frantiek. "Chalones and specific growth factors in normal and tumor growth." *Acta Universitatis Carolinae. Medica. Monographia* 110 (1984): 1.

[5] Hebda, Patricia A., et al. "Basic fibroblast growth factor stimulation of epidermal wound healing in pigs." *Journal of investigative dermatology* 95.6 (1990): 626-631.

[6] Hennings, H., K. Elgjo, and O. H. Iversen. "Delayed inhibition of epidermal DNA synthesis after injection of an aqueous skin extract (chalone)." *Virchows Archiv B* 4.1 (1969): 45-53.

[7] Martin, Paul. "Wound healing–aiming for perfect skin regeneration." *Science* 276.5309 (1997): 75-81.

[8] Mathews, John H., and Kurtis D. Fink. *Numerical methods using MATLAB*. Vol. 31. Upper Saddle River, NJ: Prentice hall, 1999.

[9] Murray, James D. "Mathematical Biology I: An Introduction, vol. 17 of Interdisciplinary Applied Mathematics." (2002).

[10] Rytmaa, T., and Kyllikki Kiviniemi. "Chloroma regression induced by the granulocytic chalone." *Nature* (1969): 995-996.

[11] Sherratt, J. A., and J. D. Murray. "Epidermal wound healing: the clinical implications of a simple mathematical model." *Cell Transplantation* 1 (1992): 365-371.

[12] Sherratt, J. A., and J. D. Murray. "Epidermal wound healing: a theoretical approach." *Comments Theor. Biol* 2.5 (1992): 315-333.

[13] Sherratt, J. A., and J. D. Murray. "Mathematical analysis of a basic model for epidermal wound healing." *Journal of mathematical biology* 29.5 (1991): 389-404.

[14] Sherratt, Jonathan A., and J. D. Murray. "Models of epidermal wound healing." *Proceedings of the Royal Society of London B: Biological Sciences* 241.1300 (1990): 29-36.

[15] Snowden, John M. "Wound closure: an analysis of the relative contributions of contraction and epithelialization." *Journal of Surgical Research* 37.6 (1984): 453-463.

[16] Van den Brenk, H. A. S. "Studies in restorative growth processes in mammalian wound healing." *British Journal of Surgery* 43.181 (1956): 525-550.

[17] Wang, Haiyan, and Shiliang Wu. "Spatial dynamics for a model of epidermal wound healing." *Mathematical biosciences and engineering: MBE* 11.5 (2014): 1215-1227.

[18] Wu, Shi-Liang, and Haiyan Wang. "Front-like entire solutions for monostable reaction-diffusion systems." *Journal of Dynamics and Differential Equations* 25.2 (2013): 505-533.

A Matlab code

A.1 Fisher-Kolmogorov equation with linear diffusion

Numerical Solutions of the 1-D Fisher-Kolmogorov Equation

$$n_t = Dn_{xx} + s * n * (1 - n)$$

Solve on the interval 0 < x < L, with initial conditions $n(x, 0) = 0$ inside the wound domain and $n(x, 0) = 1$ outside the wound domain, no flux boundary conditions at $x = 0$ and Dirichlet boundary condition of $n(x, L) = 1$ for all t.

Solve using a Forward-Euler scheme with finite difference approximations at spatial points $x_i = (i - 1) * dx$ for $i = 1, ..., N + 2$ where $(N + 1) * dx = L$.

We will find approximations to the solution of the PDE at each time step.

```
% Define and input parameters
% Note that $\lambda < 1/2$ to satisfy CFL condition.
% The code calculates an appropriate $dt$ given a lambda value.
  D = 0.001;
  s = 1.;
  L = 1.;
  N = input(' enter number of spatial points N ');
  tend = input(' enter final time tend ');
  lambda = input(' enter ratio lambda ');
  plotfreq = input(' time interval between plots ');
  tplot = min(plotfreq,tend);
  dx = L/(N+1);
  dt = lambda*(dx*dx)/D;
  b1 = D*dt/(dx*dx);
  b2 = s*dt;
  x    = dx*[0:1:N+1];
  nold = zeros(N+2,1);
  nnew = zeros(N+2,1);

% Define initial conditions
  for i=1:N+2;
      xx = x(i);
      if xx < 1.0
  nold(i) = 0.0;
      else
  nold(i) = 1.0;
      end
  end
% Plot initial conditions.
  plot(x,nold,'r*')
  hold all;
% Plot horizontal line at .8 (wound declared healed at 80% of cell density).
  nn = zeros(N+2,1);
```

```
  for i=1:N+2;
      xx = x(i);
      nn(i)=0.8;
  end
  plot(x,nn,'k:');
  hold all;

% March forward in time using Forward Euler
 t = dt;
 tcount = 0;
 while(t < tend);
    nnew(N+2) = 1;
    for i=N+1:-1:2;
         nnew(i) = nold(i)+b1*(nold(i-1)-2*nold(i)+nold(i+1))+b2*nold(i).*(1-nold(i));
    end
    nnew(1) = nold(1)+b1*(-2*nold(1)+2*nold(2))+b2*nold(1).*(1-nold(1));
    tcount = tcount+1;
    % Plot solution curves at desired timesteps.
    if(t > tplot)
        tplot = tplot+plotfreq;
        plot(x,nnew,'b-')
    end;
    % Redefine for next iteration.
    nold = nnew;
    t = t + dt;
 end;

% Plot all on same plot
 axis([0 1 0 1.2]);
 hold off;
 name = strcat('Fishers Eq: D=',num2str(D),', lambda=',num2str(lambda),',
 dx=',num2str(dx),', dt=',num2str(dt))
 xlabel('x')
 ylabel('cell density n')
 title(name)
```

A.2 Time versus wound radius graph for Fisher-Kolmogorov equation with linear diffusion

Numerical Solutions of the 1-D Fisher-Kolmogorov Equation

$$n_t = Dn_{xx} + a * n * (1 - n)$$

Solve on the interval $0 < \mathrm{x} < \mathrm{L}$, with initial conditions $n(x, 0) = 0$ inside the wound domain and $n(x, 0) = 1$ outside the wound domain, no flux boundary conditions at $x = 0$ and Dirichlet boundary condition of $n(x, L) = 1$ for all t.

Solve using a Forward-Euler scheme with finite difference approximations at spatial points $x_i = (i - 1) * dx$ for $i = 1, ..., N + 2$ where $(N + 1) * dx = L$.

We will find approximations to the solution of the PDE at each time step. We will plot a percentage of time against wound radius graph.

```
% Define and input parameters
% Note that $\lambda < 1/2$ to satisfy CFL condition.
% The code calculates an appropriate $dt$ given a lambda value.
  D = 0.001;
  a = 1.;
  L = 1.;
  N = 400;
  tend = 400;
  lambda = .25;
  plotfreq = 1;
  tplot = min(plotfreq,tend);
  dx = L/(N+1);
  dt = lambda*(dx*dx)/D;
  b1 = D*dt/(dx*dx);
  b2 = a*dt;
  x    = dx*[0:1:N+1];
  nold = zeros(N+2,1);
  nnew = zeros(N+2,1);

% Define initial conditions
  for i=1:N+2;
      xx = x(i);
      if xx < 1.0
  nold(i) = 0.0;
      else
  nold(i) = 1.0;
      end
  end

% March forward in time using Forward Euler
 t = dt;
 tcount = 0;
 for t=1:12430;
    nnew(N+2) = 1;
    for i=N+1:-1:2;
         nnew(i) = nold(i)+b1*(nold(i-1)-2*nold(i)+nold(i+1))+b2*nold(i).*(1-nold(i));
    end
    nnew(1) = nold(1)+b1*(-2*nold(1)+2*nold(2))+b2*nold(1).*(1-nold(1));
    W(t)=find(nnew>.7999,1);
    WW(t) = W(t)*(1/402);
    tcount = tcount+1;
    % Redefine for next iteration.
    nold = nnew;
 end;

% Plot time-wound radius graph
 axis([0 1 0 1.2]);
```

```
WW(12431)=0;
WWW = [0:(1/12430):1];
plot(WWW, WW, 'k-')
name = strcat('Fishers Eq:
D=',num2str(D),', lambda=',num2str(lambda),', dx=',num2str(dx),', dt=',num2str(dt))
xlabel('percentage of t')
ylabel('radius of wound')
title(name)
```

A.3 Fisher-Kolmogorov equation with nonlinear diffusion

Numerical Solutions of the 1-D Fisher-Kolmogorov Equation with Nonlinear Diffusion

$$n_t = D(n^p n_x)_x + s * n * (1 - n)$$

with $p \geq 0$.

Solve on the interval $0 < x < L$, with initial conditions $n(x, 0) = 0$ inside the wound domain and $n(x, 0) = 1$ outside the wound domain, no flux boundary conditions at $x = 0$ and Dirichlet boundary condition of $n(x, L) = 1$ for all t.

Solve using a Forward-Euler scheme with finite difference approximations at spatial points $x_i = (i - 1) * dx$ for $i = 1, ..., N + 2$ where $(N + 1) * dx = L$.

We will find approximations to the solution of the PDE at each time step.

```
% Define and input parameters
% Note that $\lambda < 1/2$ to satisfy CFL condition.
% The code calculates an appropriate $dt$ given a lambda value.
  D = 0.001;
  s = 1.;
  L = 1.;
  p = 4;
  N = input(' enter number of spatial points N ');
  tend = input(' enter final time tend ');
  lambda = input(' enter ratio lambda ');
  plotfreq = input(' time interval between plots ');
  tplot = min(plotfreq,tend);
  dx = L/(N+1);
  dt = lambda*(dx*dx)/D;
  b1 = D*dt/(dx*dx);
  b2 = s*dt;
  x    = dx*[0:1:N+1];
  nold = zeros(N+2,1);
  nnew = zeros(N+2,1);

% Define initial conditions
  for i=1:N+2;
      xx = x(i);
      if xx < 1.0
 nold(i) = 0.0;
```

```
      else
 nold(i) = 1.0;
      end
  end
% Plot initial conditions.
  plot(x,nold,'r*')
  hold all;
% Plot horizontal line at .8 (wound declared healed at 80% of cell density).
  nn = zeros(N+2,1);
  for i=1:N+2;
      xx = x(i);
      nn(i)=0.8;
  end
  plot(x,nn,'k:');
  hold all;

% March forward in time using Forward Euler
  t = dt;
  tcount = 0;
  while(t < tend);
     nnew(N+2) = 1;
     for i=N+1:-1:2;
        nnew(i) =nold(i)+b1*(((0.5*nold(i+1)+0.5*nold(i)).^p)*(nold(i+1)-nold(i))-
        ((0.5*nold(i)+0.5*nold(i-1)).^p)*(nold(i)-nold(i-1)))+b2*nold(i).*(1-nold(i));
     end
     nnew(1) = nold(1)+b1*(-2*nold(1)+2*nold(2))+b2*nold(1).*(1-nold(1));
     tcount = tcount+1;
     % Plot solution curves at desired timesteps.
     if(t > tplot)
        tplot = tplot+plotfreq;
        plot(x,nnew,'b-')
     end;
     % Redefine for next iteration.
     nold = nnew;
     t = t + dt;
 end;

% Plot all on same plot
axis([0 1 0 1.2]);
hold off;
name = strcat('NL Fishers Eq: p=',num2str(p),', D=',num2str(D),',
lambda=',num2str(lambda),', dx=',num2str(dx),', dt=',num2str(dt))
xlabel('x')
ylabel('cell density n')
title(name)
```

A.4 Time versus wound radius graph for Fisher-Kolmogorov equation with nonlinear diffusion

Numerical Solutions of the 1-D Fisher-Kolmogorov Equation with Nonlinear Diffusion

$$n_t = D(n^p n_x)_x + a * n * (1 - n)$$

with $p \geq 0$.

Solve on the interval $0 < x < L$, with initial conditions $n(x, 0) = 0$ inside the wound domain and $n(x, 0) = 1$ outside the wound domain, no flux boundary conditions at $x = 0$ and Dirichlet boundary condition of $n(x, L) = 1$ for all t.

Solve using a Forward-Euler scheme with finite difference approximations at spatial points $x_i = (i - 1) * dx$ for $i = 1, ..., N + 2$ where $(N + 1) * dx = L$.

We will find approximations to the solution of the PDE at each time step.

```
% Define and input parameters
% Note that $\lambda < 1/2$ to satisfy CFL condition.
% The code calculates an appropriate $dt$ given a lambda value.
  D = 0.001;
  a = 1.;
  L = 1.;
  p = 4;
  N = 400;
  tend = 400;
  lambda = .25;
  plotfreq = 1;
  tplot = min(plotfreq,tend);
  dx = L/(N+1);
  dt = lambda*(dx*dx)/D;
  b1 = D*dt/(dx*dx);
  b2 = a*dt;
  x    = dx*[0:1:N+1];
  nold = zeros(N+2,1);
  nnew = zeros(N+2,1);

% Define initial conditions
  for i=1:N+2;
      xx = x(i);
      if xx < 1.0
  nold(i) = 0.0;
      else
  nold(i) = 1.0;
      end
  end

% March forward in time using Forward Euler
  t = dt;
  tcount = 0;
  for t= 1:75500;
     nnew(N+2) = 1;
     for i=N+1:-1:2;
        nnew(i) = nold(i)+b1*(((0.5*nold(i+1)+0.5*nold(i)).^p)*(nold(i+1)-nold(i))-
        ((0.5*nold(i)+0.5*nold(i-1)).^p)*(nold(i)-nold(i-1)))+b2*nold(i).*(1-nold(i));
     end
```

```
     nnew(1) = nold(1)+b1*(-2*nold(1)+2*nold(2))+b2*nold(1).*(1-nold(1));
    W(t)=find(nnew>.7999,1);
    WW(t) = W(t)*(1/402);
     tcount = tcount+1;
     % Redefine for next iteration.
     nold = nnew;
 end;

% Plot all on same plot
axis([0 1 0 1.2]);
WW(75501)=0;
WWW = [0:(1/75500):1];
 plot(WWW, WW, 'k-')
name = strcat('Nonlinear Fishers Eq:
p=',num2str(p),', D=',num2str(D),', lambda=',num2str(lambda),', dx=',num2str(dx),',
dt=',num2str(dt))
 xlabel('percentage of t')
 ylabel('radius of wound')
title(name)
```

A.5 Full coupled system for activator chemical case

Numerical Solutions of the Coupled Epidermal Wound Healing System (Activator case)

$$n_t = Dn_{xx} + s(c) * n * (2 - n) - n,$$

where $D > 0$ and $s(c) = (2c_m(h - \beta) * c)/(c_m^2 + c^2) + \beta$ and

$$c_t = D_C c_{xx} + \lambda * f(n) - \lambda * c$$

where $f(n) = n(1 + \alpha^2)/(n^2 + \alpha^2)$

Initial Condition n(inside wound) $= 0, n(x, 0) = 1$. c(inside wound) $= 0, c(x, 0) = 1$.

Boundary Conditions Dirichlet at boundary, 1 is the "unwounded" value $c(1, t) = 1, n(1, t) = 1$. Neumann BC at the "origin" $c_x(0, t) = 0, n_x(0, t) = 0$.

Use a Standard FD scheme to approximate derivatives.

Use discrete approximations with spatial points $xj = (j - 1) * dx$ for $j = 1, ..., N + 2$ where $(N + 1) * dx = L$.

We want to find approximations to the solution of the PDE at the $N + 2$ points xj for $j = 1, ..., N + 2$.

```
% Define and input parameters
% Note that $\lambda < 1/2$ to satisfy CFL condition.
% The code calculates an appropriate $dt$ given a lambda value.
  D = 0.0005;
  L = 1.;
  a = 0.1; % alpha
```

```
  c_m = 40;
  h = 10;
  lambda = 30;
  D_C = 0.45;
  b = (1+c_m*c_m-2*h*c_m)/((1-c_m)*(1-c_m)); % beta
  N = input(' enter number of spatial points N ');
  tend = input(' enter final time tend ');
  CFL = input(' enter desired CFL ratio (less than 0.5) ');
  plotfreq = input(' time interval between plots ');
  tplot = min(plotfreq,tend);
  dx = L/(N+1);
  dt = CFL*(dx*dx)/D_C;
  b1 = D*dt/(dx*dx);
  b2 = D_C*dt/(dx*dx);
  x    = dx*[0:1:N+1];
  cold = zeros(N+2,1);
  cnew = zeros(N+2,1);
  nold = zeros(N+2,1);
  nnew = zeros(N+2,1);

% Define initial conditions
  for j=1:N+2;
      xx = x(j);
      if xx < 1.0
 nold(j) = 0;
 cold(j) = 0;
      else
 nold(j) = 1.0;
 cold(j) = 1.0;
      end
  end
 % Plot horizontal line at .8 (wound declared healed at 80% of cell density).
  nn = zeros(N+2,1);
  for j=1:N+2;
    xx = x(j);
    nn(j)=0.8;
    end
  plot(x,nn,'k:');
  hold all;
% Define s(c) function.
   s = @(x) (2*c_m*(h-b)*x)/(c_m*c_m+x*x)+b;
% Define f(n) function.
   f = @(x) (x*(1+a*a))/(x*x+a*a);

% March forward in time using Forward Euler
  t = dt;
  tcount = 0;
  while(t < tend);
  % Set right-hand boundary condition (Dirichlet).
    cnew(N+2) = 1.;
    nnew(N+2) = 1.;
```

```
%  March forward in time.
    for j = N+1:-1:2;
        nnew(j) = nold(j) + b1*(nold(j-1)-2*nold(j)+nold(j+1))+
        dt*s(cold(j))*nold(j).*(2-nold(j))-nold(j)*dt;
        cnew(j) = cold(j) + b2*(cold(j-1)-2*cold(j)+cold(j+1))+
        dt*lambda*(f(nnew(j))-cold(j));
    end
 % Set left-hand boundary condition (Neumann).
     nnew(1) = nold(1) + b1*(-2*nold(1)+2*nold(2))+
          dt*s(cold(1))*nold(1)*(2-nold(1))-nold(1)*dt;
 cnew(1) = cold(1) + b2*(-2*cold(1)+2*cold(2))+
          dt*lambda*(f(nold(1))-cold(1));

    tcount = tcount+1;
  % Plot solution curves.
      if(t > tplot)
         tplot = tplot+plotfreq;
         plot(x,nnew,'g-')
         plot(x,cnew,'b-')
      end;
   % Redefine for next iteration.
    nold = nnew;
    cold = cnew;
    t = t + dt;
  end;

% Plot all on same plot
axis([0 1 0 1.5]);
hold off;
name = strcat('Coupled Wound Healing System:
CFL=',num2str(CFL),', dx=',num2str(dx),', dt=',num2str(dt))
xlabel('x')
ylabel('cell density n/ chemical concentration c')
title(name)
```

A.6 Time versus wound radius graph for full coupled system for activator chemical case

$$n_t = Dn_{xx} + s(c) * n * (2 - n) - n,$$

where $D > 0$ and $s(c) = (2c_m(h - \beta) * c)/(c_m^2 + c^2) + \beta$ and

$$c_t = D_C c_{xx} + \lambda * f(n) - \lambda * c$$

where $f(n) = n(1 + \alpha^2)/(n^2 + \alpha^2)$

Initial Condition n(inside wound) $= 0, n(x, 0) = 1$. c(inside wound) $= 0, c(x, 0) = 1$.

Boundary Conditions Dirichlet at boundary, 1 is the "unwounded" value $c(1, t) = 1, n(1, t) = 1$. Neumann BC at the "origin" $c_x(0, t) = 0, n_x(0, t) = 0$.

Use a Standard FD scheme to approximate derivatives.

Use discrete approximations with spatial points $xj = (j-1) * dx$ for $j = 1, ..., N+2$ where $(N+1) * dx = L$.

We want to find approximations to the solution of the PDE at the $N+2$ points xj for $j = 1, ..., N+2$.

```
% Define and input parameters
% Note that $\lambda < 1/2$ to satisfy CFL condition.
% The code calculates an appropriate $dt$ given a lambda value.
  D = 0.0005;
  L = 1.;
  a = 0.1; % alpha
  c_m = 40;
  h = 10;
  lambda = 30;
  D_C = 0.45;
  b = (1+c_m*c_m-2*h*c_m)/((1-c_m)*(1-c_m)); % beta
  N = 90;
  tend = 90;
  CFL = .25;
  plotfreq = 1;
  tplot = min(plotfreq,tend);
  dx = L/(N+1);
  dt = CFL*(dx*dx)/D_C;
  b1 = D*dt/(dx*dx);
  b2 = D_C*dt/(dx*dx);
  x    = dx*[0:1:N+1];
  cold = zeros(N+2,1);
  cnew = zeros(N+2,1);
  nold = zeros(N+2,1);
  nnew = zeros(N+2,1);

% Define initial conditions
  for j=1:N+2;
      xx = x(j);
      if xx < 1.0
 nold(j) = 0;
 cold(j) = 0;
      else
 nold(j) = 1.0;
 cold(j) = 1.0;
      end
  end
% Define s(c) function.
   s = @(x) (2*c_m*(h-b)*x)/(c_m*c_m+x*x)+b;
% Define f(n) function.
   f = @(x) (x*(1+a*a))/(x*x+a*a);
%% March forward in time using Forward Euler
 for t = 1:326361;
  % Set right-hand boundary condition (Dirichlet).
```

```
    cnew(N+2) = 1.;
    nnew(N+2) = 1.;
%  March forward in time.
    for j = N+1:-1:2;
        nnew(j) = nold(j) + b1*(nold(j-1)-2*nold(j)+nold(j+1))+
        dt*s(cold(j))*nold(j).*(2-nold(j))-nold(j)*dt;
        cnew(j) = cold(j) + b2*(cold(j-1)-2*cold(j)+cold(j+1))+
        dt*lambda*(f(nnew(j))-cold(j));
    end
 % Set left-hand boundary condition (Neumann).
     nnew(1) = nold(1) + b1*(-2*nold(1)+2*nold(2))+
     dt*s(cold(1))*nold(1)*(2-nold(1))-nold(1)*dt;
 cnew(1) = cold(1) + b2*(-2*cold(1)+2*cold(2))+
 dt*lambda*(f(nold(1))-cold(1));

    W(t)=find(nnew>.7999,1);
    WW(t) = W(t)*(1/92);
   % Redefine for next iteration.
    nold = nnew;
    cold = cnew;
  end;

% Plot
WW(326362)=0;
WWW = [0:(1/326361):1];
% Plot(WWW, WW, 'k-')
axis([0 1 0 1]);
name = strcat('Coupled Wound Healing System: CFL=',num2str(CFL),',
dx=',num2str(dx),', dt=',num2str(dt))
xlabel('percentage of t')
ylabel('radius of wound')
title(name)
```

A.7 Full coupled system for inhibitor chemical case

Numerical Solutions of the Coupled Epidermal Wound Healing System (Inhibitor case)

$$n_t = Dn_{xx} + s(c) * n * (2 - n) - n,$$

where $D > 0$ and $s(c) = (((h-1)*c+h)/(2*(h-1)*c+1))$ and

$$c_t = D_C c_{xx} + \lambda * f(n) - \lambda * c$$

where $f(n) = n$
Initial Condition n(inside wound) $= 0, n(x,0) = 1.c$(inside wound)$= 0, c(x,0) = 1.$

Boundary Conditions Dirichlet at boundary, 1 is the "unwounded" value $c(1,t) = 1, n(1,t) = 1$. Neumann BC at the "origin" $c_x(0,t) = 0, n_x(0,t) = 0$.

Use a Standard FD scheme to approximate derivatives.

Use discrete approximations with spatial points $xj = (j-1) * dx for j = 1, ..., N+2$ where $(N+1) * dx = L$.

We want to find approximations to the solution of the PDE at the $N + 2$points $xj$for$j = 1, ..., N + 2$.

```
% Define and input parameters
% Note that $\lambda < 1/2$ to satisfy CFL condition.
% The code calculates an appropriate $dt$ given a lambda value.
  D = 0.0001;
  L = 1.;
  h = 10;
  lambda = 5;
  D_C = 0.85;
  N = input(' enter number of spatial points N ');
  tend = input(' enter final time tend ');
  CFL = input(' enter desired CFL ratio (less than 0.5) ');
  plotfreq = input(' time interval between plots ');
  tplot = min(plotfreq,tend);
  dx = L/(N+1);
  dt = CFL*(dx*dx)/D_C;
  b1 = D*dt/(dx*dx);
  b2 = D_C*dt/(dx*dx);
  x    = dx*[0:1:N+1];
  cold = zeros(N+2,1);
  cnew = zeros(N+2,1);
  nold = zeros(N+2,1);
  nnew = zeros(N+2,1);

% Define initial conditions
  for j=1:N+2;
      xx = x(j);
      if xx < 1.0
 nold(j) = 0;
 cold(j) = 0;
      else
 nold(j) = 1.0;
 cold(j) = 1.0;
      end
  end
  % Plot horizontal line at .8 (wound declared healed at 80% of cell density).
  nn = zeros(N+2,1);
  for j=1:N+2;
    xx = x(j);
    nn(j)=0.8;
    end
  plot(x,nn,'k:');
  hold all;
% Define s(c) function.
   s = @(x) (((h-1)*x+h)/(2*(h-1)*x+1));
% Define f(n) function.
   f = @(x) (x);
```

```
% March forward in time using Forward Euler
  t = dt;
  tcount = 0;
  while(t < tend);
  % Set right-hand boundary condition (Dirichlet).
    cnew(N+2) = 1.;
    nnew(N+2) = 1.;
%  March forward in time.
    for j = N+1:-1:2;
        nnew(j) = nold(j) + b1*(nold(j-1)-2*nold(j)+nold(j+1))+
        dt*s(cold(j))*nold(j).*(2-nold(j))-nold(j)*dt;
        cnew(j) = cold(j) + b2*(cold(j-1)-2*cold(j)+cold(j+1))+
        dt*lambda*(f(nnew(j))-cold(j));
    end
  % Set left-hand boundary condition (Neumann).
nnew(1) = nold(1) + b1*(-2*nold(1)+2*nold(2))+ dt*s(cold(1))*nold(1)*(2-nold(1))-
nold(1)*dt;
cnew(1) = cold(1) + b2*(-2*cold(1)+2*cold(2))+ dt*lambda*(f(nold(1))-cold(1));


    tcount = tcount+1;
   % Plot solution curves.
      if(t > tplot)
         tplot = tplot+plotfreq;
         plot(x,nnew,'g-')
         plot(x,cnew,'b-')
      end;
    % Redefine for next iteration.
    nold = nnew;
    cold = cnew;
    t = t + dt;
  end;

% Plot all on same plot
axis([0 1 0 1.5]);
hold off;
name = strcat('Nonlinear Coupled Fishers Eq:
CFL=',num2str(CFL),', dx=',num2str(dx),', dt=',num2str(dt))
xlabel('x')
ylabel('cell density n/chemcial concentration c')
title(name)
```

A.8 Time versus wound radius graph for full coupled system for inhibitor chemical case

$$n_t = Dn_{xx} + s(c) * n * (2 - n) - n,$$

where $D > 0$ and $s(c) = (((h-1) * c + h)/(2 * (h-1) * c + 1))$ and

$$c_t = D_C c_{xx} + \lambda * f(n) - \lambda * c$$

where $f(n) = n$

Initial Condition $n(\text{inside wound}) = 0, n(x,0) = 1.c(\text{inside wound}) = 0, c(x,0) = 1.$

Boundary Conditions Dirichlet at boundary, 1 is the "unwounded" value $c(1,t) = 1, n(1,t) = 1$. Neumann BC at the "origin" $c_x(0,t) = 0, n_x(0,t) = 0.$

Use a Standard FD scheme to approximate derivatives.

Use discrete approximations with spatial points $xj = (j-1) * dx for j = 1, ..., N+2$ where $(N+1) * dx = L.$

We want to find approximations to the solution of the PDE at the $N+2$points $xj$for$j = 1, ..., N+2.$

```
% Define and input parameters
% Note that $\lambda < 1/2$ to satisfy CFL condition.
% The code calculates an appropriate $dt$ given a lambda value.
  D = 0.0001;
  L = 1.;
  h = 10;
  lambda = 5;
  D_C = 0.85;
  N = 65;
  tend = 65;
  CFL = .25;
  plotfreq = 1;
  tplot = min(plotfreq,tend);
  dx = L/(N+1);
  dt = CFL*(dx*dx)/D_C;
  b1 = D*dt/(dx*dx);
  b2 = D_C*dt/(dx*dx);
  x    = dx*[0:1:N+1];
  cold = zeros(N+2,1);
  cnew = zeros(N+2,1);
  nold = zeros(N+2,1);
  nnew = zeros(N+2,1);

% Define initial conditions
  for j=1:N+2;
      xx = x(j);
      if xx < 1.0
 nold(j) = 0;
 cold(j) = 0;
      else
 nold(j) = 1.0;
 cold(j) = 1.0;
      end
  end
% Define s(c) function.
   s = @(x) (((h-1)*x+h)/(2*(h-1)*x+1));
% Define f(n) function.
```

```
   f = @(x) (x);

% March forward in time using Forward Euler
  t = dt;
  tcount = 0;
  for t = 1:543088;
  % Set right-hand boundary condition (Dirichlet).
    cnew(N+2) = 1.;
    nnew(N+2) = 1.;
%  March forward in time.
    for j = N+1:-1:2;
        nnew(j) = nold(j) + b1*(nold(j-1)-2*nold(j)+nold(j+1))+
        dt*s(cold(j))*nold(j).*(2-nold(j))-nold(j)*dt;
        cnew(j) = cold(j) + b2*(cold(j-1)-2*cold(j)+cold(j+1))+
        dt*lambda*(f(nnew(j))-cold(j));
    end
  % Set left-hand boundary condition (Neumann).
     nnew(1) = nold(1) + b1*(-2*nold(1)+2*nold(2))+
     dt*s(cold(1))*nold(1)*(2-nold(1))-nold(1)*dt;
 cnew(1) = cold(1) + b2*(-2*cold(1)+2*cold(2))+
 dt*lambda*(f(nold(1))-cold(1));

    W(t)=find(nnew>.7999,1);
    WW(t) = W(t)*(1/67);

    % Redefine for next iteration.
    nold = nnew;
    cold = cnew;
  end;
 % Plot all on same plot
 WW(543089)=0;
 WWW = [0:(1/543088):1];
 plot(WWW, WW, 'k-')
 axis([0 1 0 1]);
name = strcat('Nonlinear Coupled Fishers Eq: CFL=',num2str(CFL),',
dx=',num2str(dx),', dt=',num2str(dt))
xlabel('percentage of t')
ylabel('radius of wound')
title(name)
```

B Calculation of $s(c_0) = k$ for activator chemical case in coupled model

$$
\begin{aligned}
s(c_0) &= k \cdot \Big[\frac{2c_m(h - \frac{c_0^2+c_m^2-2hc_0c_m}{(c_0-c_m)^2})c_0}{c_m^2+c_0^2} + \frac{c_0^2+c_m^2-2hc_0c_m}{(c_0-c_m)^2}\Big], \\
&= k \cdot \Big[\frac{2hc_0c_m - \frac{2c_0^3c_m+2c_0c_m^3-4hc_0^2cm^2}{(c_0-c_m)^2}}{c_m^2+c_0^2} + \frac{c_0^2+c_m^2-2hc_0c_m}{(c_0-c_m)^2}\Big], \\
&= \Big[k \cdot \frac{2hc_0c_m}{c_m^2+c_0^2} - \frac{2c_0^3c_m+2c_0c_m^3-4hc_0^2cm^2}{(c_m^2+c_0^2)(c_0-c_m)^2} + \frac{c_0^2+c_m^2-2hc_0c_m}{(c_0-c_m)^2}\Big], \\
&= k \cdot \Big[\frac{2hc_0c_m(c_0-c_m)^2}{(c_m^2+c_0^2)(c_0-c_m)^2} - \frac{2c_0^3c_m+2c_0c_m^3-4hc_0^2cm^2}{(c_m^2+c_0^2)(c_0-c_m)^2} + \frac{(c_0^2+c_m^2-2hc_0c_m)(c_m^2+c_0^2)}{(c_m^2+c_0^2)(c_0-c_m)^2}\Big], \\
&= k \cdot \Big[\frac{2hc_0c_m(c_0^2+c_m^2-2c_0c_m)}{(c_m^2+c_0^2)(c_0-c_m)^2} - \frac{2c_0^3c_m+2c_0c_m^3-4hc_0^2cm^2}{(c_m^2+c_0^2)(c_0-c_m)^2} + \frac{(c_0^2+c_m^2-2hc_0c_m)(c_m^2+c_0^2)}{(c_m^2+c_0^2)(c_0-c_m)^2}\Big], \\
&= k \cdot \Big[\frac{2hc_0^3c_m+2hc_0c_m^3-4hc_0^2c_m^2-2c_0^3c_m-2c_0c_m^3+4hc_0^2c_m^2}{(c_m^2+c_0^2)(c_0-c_m)^2} \\
&+ \frac{c_0^2c_m^2+c_0^4+c_m^4+c_0^2c_m^2-2hc_0c_m^3-2hc_0^3c_m}{(c_m^2+c_0^2)(c_0-c_m)^2}\Big], \\
&= k \cdot \frac{-2c_0^3c_m-2c_0c_m^3+c_0^2c_m^2+c_0^4+c_m^4+c_0^2c_m^2}{(c_m^2+c_0^2)(c_0-c_m)^2}, \\
&= k \cdot \frac{c_0^4+c_m^4-2c_0^3c_m-2c_0c_m^3+2c_0^2c_m^2}{(c_m^2+c_0^2)(c_0^2+c_m^2-2c_0c_m)}, \\
&= k \cdot \frac{c_0^4+c_m^4-2c_0^3c_m-2c_0c_m^3+2c_0^2c_m^2}{c_0^4+c_m^4-2c_0^3c_m-2c_0c_m^3+2c_0c_m}, \\
&= k \cdot (1) = k.
\end{aligned}
$$

C Wang and Wu general results on reaction-diffusion equations

Let a general reaction-diffusion system be given by

$$u_t = Du_{xx} + g(u) \text{ for } x \in \mathbb{R}, t \geq 0. \tag{52}$$

with

$$u(x,0) = u_0(x) \text{ for } x \in \mathbb{R}, \tag{53}$$

where $u = (u_1), D = \text{diag}(d_1, d_2, ..., d_N), d_i > 0$ for $i = 1, ..., N$ and $g(u) = (g_1(u), g_2(u), ..., g_N(u))$ and u_0 is a bounded uniformly continuous function on $\mathbb{R}$.

H_1
i. Assume that $D = \text{diag}(d_1, d_2, ..., d_N), d_i > 0$ for $i = 1, ..., N$. Let $k^+ = (k_i^+) \gg 0$ and $g : [0, k^+] \to \mathbb{R}^N$ be a continuous and twice piecewise continuously differentiable function. Assume that C_{k^+} is an invariant set of Equation (52) in the sense that for any given $u_0 \in C_{k^+}$, the solution of Equation (52) with the initial condition u_0 exists and remains in C_{k^+} for $t \in [0, \infty)$.

ii. Let $0 \ll k^- = (k_i^-) \leq k = (k_i) \leq k^+$. Assume there exists continuous and twice piecewise continuously differentiable functions $g^{\pm} = (g_i^{\pm}) : [0, k^+] \to \mathbb{R}^N$ such that for $u \in [0, k^+]$

$$g^-(u) \leq g(u) \leq g^+(u).$$

iii. $g(0) = g(k) = 0$ and there is no other positive equilibrium of g between 0 and k. $g^{\pm}(0) = g^{\pm}(k^{\pm}) = 0$. There is no other positive equilibrium of $g^{\pm}$ between 0 and $k^{\pm}$. g has a finite number of number of equilibria in $[0, k^+]$.

iv. For each non-cooperative reaction-diffusion equation there exists a cooperative system

$$u_t = Du_{xx} + g^+(u) \text{ for } x \in \mathbb{R}, t \geq 0 \tag{54}$$
$$u_t = Du_{xx} + g^-(u) \text{ for } x \in \mathbb{R}, t \geq 0 \tag{55}$$

where g^+ lies above g and g^- lies below g.

v. Equations (54) and (55) have the same Jacobian matrix $g'(0)$ at $u = 0$.

H_2
Assume that A_Λ with irreducible blocks is in block lower triangular form. Further assume that its first diagonal block has the positive principal eigenvalue $M(A_\Lambda)$ and $M(A_\Lambda)$ is strictly larger than the principal eigenvalues of all other irreducible diagonal blocks for $\Lambda \geq 0$. In addition, assume that there is a positive eigenvector $v_\Lambda = (v_\Lambda^i) \gg 0$ of A_Λ corresponding to $M(A_\Lambda)$, and that v_Λ is continuous with respect to Λ for $\Lambda > 0$.

H_3
Assume that for any $\eta > 0, \Lambda \in [0, \Lambda*]$,

$$g^+(\eta v_\Lambda) \leq \eta g'(0) v_\Lambda, \text{ where } v_\Lambda = (v_\Lambda^i).$$

Theorem 2. *Assume $(H_1), (H_2)$, and (H_3) hold. Then the following statements are valid: (i) For any $u_0 \in C_k$ with compact support, the solution $u(x,t)$ of Equations (52) and (53) satisfies*

$$\lim_{t\to\infty} \sup_{|x|\geq tc} u(x,t) = 0, \text{ for } c > c^*.$$

(ii) For any vector $\omega \in \mathbb{R}^N, \omega \gg 0$, there is a positive R_ω with the property that if $u_0 \in C_k$ and $u_0 \geq \omega$ on an interval of length $2R_\omega$, then the solution $u(x,t)$ of Equations (52) and (53) satisfies

$$k^- \leq \liminf_{t\to\infty} \inf_{|x|\leq tc} u(x,t) \leq k^+, \text{ for } 0 < c < c^*.$$

(iii) For each $c > c^*$, Equation (52) admits a traveling wave solution $\phi(x + ct)$ such that $0 \ll \phi(\xi) \leq k^+, \xi \in \mathbb{R}$,

$$k^- \leq \liminf_{\xi\to\infty} \phi(\xi) \leq \limsup_{\xi\to\infty} \phi(\xi) \leq k^+$$

and

$$\lim_{\xi\to-\infty}\phi(\xi)e^{-\Lambda_1(c)\xi}=v_{\lambda_1}.$$

If, in addition Equation (52) is cooperative in C_k, then u is nondecreasing on $\mathbb{R}$.

(iv.) For $c=c^*$, Equation (52) admits a nonconstant traveling wave solution $\phi(x+ct)$ such that $0\le\phi(\xi)\le k^+,\xi\in\mathbb{R}$.

(v.) For $0<c<c^*$ Equation (52) does not admit a traveling wave solution $\phi(x+ct)$ with $\liminf_{\xi\to\infty}\phi(\xi)\gg 0$ and $\phi(-\infty)=0$.